

Population-based learning in simple stochastic games

Scott Merrill¹ and Alex McAvoy^{2,3,*}

¹Department of Computer Science, University of North Carolina at Chapel Hill, Chapel Hill, NC

²School of Data Science and Society, University of North Carolina at Chapel Hill, Chapel Hill, NC

³Department of Mathematics, University of North Carolina at Chapel Hill, Chapel Hill, NC

December 30, 2025

Abstract

Conflicts of interest are ubiquitous in populations. When individuals interact, there are often discrepancies between what is best for the individual and what is best for the larger group. Social dilemmas capture the differing incentives between individuals and groups, and specific models like the prisoner’s dilemma have been studied extensively in both evolutionary game theory and multi-agent reinforcement learning. However, at the intersection of these fields lies the understudied question of how population-level stochasticity affects collective learning dynamics and emergent behaviors. In this work, we study the impact of random interactions in populations of greedy (purely self-interested) agents by examining simple, mixed-motivation stochastic games. Despite the fact that naive self-play leads to inefficient outcomes in cooperative social dilemmas, we find that stochasticity in interaction partners within a population can reverse these outcomes, leading to much larger rewards, on average. This behavior is consistent across a variety of social dilemmas, and it suggests that transient (rather than stable) encounters can serve as a mechanism for eliciting prosocial behaviors in a population, even when all agents are self-interested.

1 Introduction

Multi-agent reinforcement learning (MARL) involves modeling and training autonomous agents that interact within a shared environment. In many real-world systems, agents operate independently, without access to centralized control, global reward signals, or direct communication (apart from reward signals obtained from interaction). Such decentralized settings are common in applications including autonomous vehicles navigating shared roadways [1, 2], algorithmic traders in financial markets [3, 4], distributed energy management systems [5, 6], and communication networks managed by self-interested service providers [7]. In these environments, each agent typically maximizes its own individual reward, without regard for the goals, strategies, or learning processes of others. This form of selfish optimization, where agents update their policies to improve only their personal return, presents significant challenges for achieving globally efficient outcomes.

*Please direct correspondence to A.M. (amcavoy@unc.edu).

28 These challenges are especially pronounced in social dilemmas, a class of multi-agent problems
29 characterized by a conflict between individual incentives and collective welfare. In a social
30 dilemma, agents face a choice between defection (a strategy that yields higher personal reward at
31 the expense of others) and cooperation (a strategy that may incur short-term individual costs but
32 produces greater overall benefit when adopted widely). Classic examples include the prisoner’s
33 dilemma, the public goods game, and the tragedy of the commons. When all agents pursue
34 their narrow self-interest, the population often converges to Pareto-suboptimal equilibria, where
35 mutual defection dominates despite the availability of mutually beneficial cooperative strategies.

36 Social dilemmas are important to study both theoretically and practically. They model a wide
37 array of real-world challenges, such as traffic congestion, resource depletion, climate action, and
38 public health compliance, where the lack of coordination among autonomous agents leads to in-
39 efficient or even catastrophic outcomes. Addressing these coordination failures is a fundamental
40 problem in multi-agent systems.

41 To date, the predominant approaches for fostering cooperation in MARL rely on centralized
42 mechanisms, including shared objectives, joint training procedures, engineered reward shaping,
43 or communication protocols. While effective in controlled settings, these methods often assume
44 access to centralized observability, joint optimization, or structured communication which are
45 rarely available in practice. In contrast, decentralized MARL considers the more realistic setting
46 in which agents learn independently, act without coordination, and optimize selfishly. This
47 formulation better captures real-world conditions, yet cooperation remains difficult to achieve
48 under such constraints.

49 One proposed solution is to leverage random encounters, where agents interact randomly
50 with others drawn from the population and update their strategies based on the outcomes of
51 those interactions. This setup introduces strategic diversity by exposing agents to a wide range of
52 behaviors over time, without requiring persistent partners or structured coordination. However,
53 prior work has largely concluded that random encounters alone are insufficient for sustaining co-
54 operation. In response, studies have proposed additional mechanisms, such as partner selection,
55 interaction opt-out, or reputation systems, to stabilize cooperative behavior. These mechanisms
56 often rely on assumptions such as agent memory, observability of others’ behavior, or control
57 over the interaction structure, conditions that may not hold in fully decentralized systems.

58 This study revisits the role of random encounters in decentralized MARL and presents evi-
59 dence that randomized partner interactions can, in fact, promote cooperation, even among selfish
60 agents. Using Markov games that retain the core structure of social dilemmas it is shown that
61 random encounters introduce population-level stochasticity that can help escape defective equi-
62 libria and discover globally optimal strategies. This finding runs counter to the prevailing view
63 that randomness in interactions inherently drives populations toward mutual defection.

64 A central insight is the role of forgiving strategies in enabling cooperative dynamics. Forgiv-
65 ing agents respond to defection not with retaliation, but with continued cooperation, tolerating
66 short-term exploitation in exchange for long-term benefits. While seemingly vulnerable, these
67 strategies can act as stabilizers in population dynamics, guiding selfish agents toward coopera-
68 tive equilibria by creating a path back to mutual benefit. Their spontaneous emergence highlights
69 the importance of population diversity and raises the question of whether such strategies can be
70 deliberately introduced into learning populations to improve outcomes.

71 To better understand and track these dynamics, a novel representation learning framework is
72 introduced: the behavior space autoencoder (BSAE). This method constructs a low-dimensional

73 latent space that captures agent behaviors, enabling visualization, measurement, and analysis
74 of population trajectories over the course of learning. Beyond diagnostics, this behavior space
75 supports latent reinforcement learning, allowing policies to be directly optimized in the behav-
76 ior space. This approach yields substantial improvements in sample efficiency and provides a
77 powerful tool for steering population-level learning dynamics.

78 Together, these results demonstrate that cooperation can emerge in decentralized systems
79 composed of selfish learners, even in the absence of communication, memory, or central con-
80 trol. Through random interactions and diverse policy landscapes, agents can self-organize into
81 globally cooperative outcomes. This challenges long-standing assumptions in the MARL liter-
82 ature and opens new avenues for designing decentralized systems capable of resolving social
83 dilemmas.

84 2 Related Work

85 **Game theory and multi-agent reinforcement learning.** Game theory provides mathematical
86 tools to analyze multi-agent interactions and has been used extensively in MARL research to
87 study equilibrium concepts like Nash Equilibria and correlated equilibria [8]. While MARL re-
88 search often centers on temporally and spatially extended environments and specialized bench-
89 marks [9] (e.g., StarCraft II, Quake III), other efforts seek more general insights into multi-agent
90 learning in smaller-scale social dilemmas [10–12]. These connections have been further explored
91 in works [13] establishing formal frameworks for agent interactions.

92 **Social dilemmas.** In social dilemmas [14], including the prisoner’s dilemma and public goods
93 games, individual incentives are at odds with collective welfare, leading to conflicts of interest.
94 In repeated or Markov-game formulations, agents can learn strategies conditioned on past states
95 and actions, leading to a wealth of possible equilibria. Classic findings show that naive self-
96 play often leads to defection, though specialized reward shaping [15, 16], partner choices [17,
97 18] communication [19], or carefully tuned learning rates [`learningRateVsreward`, 20, 21] can
98 sometimes restore cooperation [22–25].

99 **Population-based learning.** Population-based methods typically train multiple agents in par-
100 allel, often saving strategies along a training trajectory [26]. Our work is closely related but
101 emphasizes random interaction partners each round and focuses on social dilemmas. Crucially,
102 the goal is to lift the entire population to cooperative rewards, not just a single agent, without
103 the use of institutions or other centralized control. The closest work to this study uses exact
104 calculations in matrix games in conjunction with a partial differential equation to study collec-
105 tive learning in effectively infinite populations [27]. There, it is noted that random interactions
106 can change outcomes relative to learning in pairs, but the primary strategy space is the two-
107 dimensional space of reactive strategies, which cannot accommodate multi-state games and even
108 yields a limited behavioral space within matrix games.

109 **Population-based learning in social dilemmas.** The prevailing view in the literature holds that
110 population-based learning and random encounters are insufficient to overcome selfish behavior
111 in social dilemmas. Previous studies have introduced additional mechanisms, such as partner

112 selection and the ability to opt out of interactions, as critical for enabling cooperation. For example, [28] propose a reactive partner selection mechanism. In each round, agents select a partner
113 for a one-shot prisoner’s dilemma game and update their strategies using Q-learning. The study
114 finds that cooperation can emerge when agents learn policies for partner selection; however, they
115 find random partner selection strategies lead to widespread defection.

116 A similar investigation by [29] explores a setting in which agents may opt out of interactions.
117 Again employing Q-learning, the study shows that allowing agents to learn opt-out strategies
118 fosters cooperation. Consistent with the findings of [28], this study also concludes that random
119 interactions result in defective outcomes.

120 Collectively, prior studies suggest that random encounters tend to produce inefficient out-
121 comes in social dilemmas. However, the findings presented in this work challenge this narrative.
122 Evidence is provided that a more general form of population-based learning, absent mechanisms
123 such as engineered partner selection or opt-out options, can lead to the reversal of defection and
124 the emergence of cooperation across a wide spectrum of social dilemmas. This suggests that the
125 lack of cooperative outcomes reported in earlier work may not be an inherent limitation of popu-
126 lation dynamics, but rather a consequence of specific experimental design choices. These include
127 the reliance on Q-learning, the restriction to single-shot interactions, or an insufficient number of
128 training episodes. These results hold important implications for the design and interpretation of
129 multi-agent learning systems.

131 3 Model

132 3.1 Markov decision processes

133 A Markov decision processes (MDP) is a mathematical framework for modeling sequential decision-
134 making tasks involving a single agent operating within a probabilistic environment. Formally,
135 an MDP can be defined as a tuple (S, A, r, P, γ) , where:

- 136 • S is the *state space*, representing all possible configurations or situations of the environment.
137 Each $s \in S$ corresponds to a specific, fully observable condition of the environment.
- 138 • A is the *action space*, which consists of all possible actions the agent can take. The available
139 actions may depend on the current state.
- 140 • $r : S \times A \rightarrow \mathbb{R}$ is the *reward function*, which maps a state-action pair to a scalar reward value.
141 This function quantifies the immediate benefit or cost to the agent of taking a specific action
142 in a given state.
- 143 • $P : S \times A \rightarrow \Delta(S)$ is the *transition probability function*, where $\Delta(S)$ denotes the set of proba-
144 bility distributions over S . Specifically, $P(s' | s, a)$ represents the probability of transitioning
145 to state s' when the agent takes action a in state s .
- 146 • $\gamma \in [0, 1]$ is the *discount factor*, which determines the present value of future rewards. A
147 lower γ indicates a preference for short-term rewards, while a higher γ values long-term
148 rewards more heavily.

149 An agent interacting with an MDP selects actions according to a strategy $\pi : S \rightarrow \Delta(A)$,
150 which maps states to a distribution over actions. The agent’s objective is to identify a strategy

151 that maximizes the expected cumulative discounted reward, which can be formally expressed as:

$$\mathbb{E}_\pi \left[\sum_{t=0}^{\infty} \gamma^t r(s_t, a_t) \right], \quad (1)$$

152 where $s_0 \in S$ is the initial state, $a_t \sim \pi(\cdot | s_t)$, and $s_{t+1} \sim P(\cdot | s_t, a_t)$ for $t \geq 0$.

153 3.2 Markov games

154 Markov games, also known as stochastic games, extend Markov Decision Processes (MDPs) to
155 settings involving multiple agents, enabling the study of strategic interaction in shared, stochastic
156 environments [30]. A Markov game with n agents can be described by the tuple:

$$(S, \{A_i\}_{i=1}^n, \{r_i\}_{i=1}^n, P, \gamma). \quad (2)$$

157 where the state space S and the discount factor γ retain the same meaning as in the MDP frame-
158 work. The multi-agent extension introduces agent-specific action sets, individualized reward
159 functions, and a joint influence on the environment dynamics:

- 160 • Each agent $i \in \{1, \dots, n\}$ has its own action space A_i , from which it selects actions inde-
161 pently at each time step.
- 162 • The reward function $r_i : S \times A_1 \times \dots \times A_n \rightarrow \mathbb{R}$ defines agent-specific rewards based on
163 the current state and the joint actions of all agents.
- 164 • The transition function $P(s' | s, a_1, \dots, a_n)$ describes how the environment evolves given the
165 joint actions of all agents.

166 At each time step, agents choose their actions simultaneously, resulting in a joint action profile
167 (a_1, \dots, a_n) . The system then transitions to a new state based on P , and each agent i receives a
168 reward r_i . Each agent aims to maximize its expected cumulative discounted reward:

$$\mathbb{E}_\pi \left[\sum_{t=0}^{\infty} \gamma^t r_i(s_t, a_{1,t}, \dots, a_{n,t}) \right], \quad (3)$$

169 where $\pi = (\pi_1, \dots, \pi_n)$ is the joint strategy profile.

170 In contrast to single-agent MDPs, Markov games introduce multiple agents whose simultane-
171 ous and potentially conflicting objectives transform the environment into a dynamic and strategic
172 setting. Each agent must account not only for environmental dynamics but also for the evolving
173 behavior of others. This multi-agent formulation enables the modeling of complex strategic in-
174 teractions, such as competition, cooperation, and coordination, making it a powerful framework
175 for analyzing decision-making in shared environments.

176 3.3 Social dilemmas

177 A social dilemma describes a scenario where individually rational decisions produce outcomes
178 that are collectively inefficient or even harmful. More formally, it arises when the incentives of
179 each agent align with actions that maximize personal benefit, yet when all agents act on these

180 incentives, the resulting joint outcome is worse for everyone than if they had coordinated differ-
181 ently. This creates a core tension between optimizing for self-interest and achieving outcomes
182 that are beneficial for the group as a whole.

183 Social dilemmas are central to understanding cooperation and coordination challenges in
184 multi-agent systems. They appear across a wide range of real-world domains. In environmental
185 economics, for example, climate change mitigation presents a classic dilemma: individual ac-
186 tors, such as countries or corporations, may benefit from continuing to emit greenhouse gases,
187 avoiding the short-term costs of abatement. Yet, when all actors behave this way, the long-term
188 global consequences are catastrophic. Similarly, in public goods provision, individuals may be
189 tempted to withhold contributions while benefiting from others' efforts, ultimately leading to
190 underfunding or collapse of the shared resource.

191 In the context of autonomous systems, social dilemmas present a growing challenge. Con-
192 sider self-driving vehicles navigating a four-way stop. Each car has an incentive to proceed
193 quickly to minimize delay. If one vehicle yields while others proceed, the system functions
194 smoothly. But if all vehicles attempt to go first, collisions or deadlock can occur, degrading traffic
195 flow and safety for everyone. Similarly, during lane merging or highway ramp access, vehicles
196 that aggressively merge to minimize travel time may cause stop-and-go traffic or increase the risk
197 of accidents. In contrast, systems that incorporate occasional yielding or cooperative timing can
198 improve overall efficiency, though these behaviors are not individually optimal in the short term.

199 These examples illustrate why social dilemmas are critical to study: they capture the essential
200 tension between local decision-making and global outcomes. Designing agents that can recognize
201 and navigate such tradeoffs is a key challenge in multi-agent learning, especially in domains
202 where safety, fairness, and efficiency depend on sustained coordination. Understanding the
203 mechanisms that enable cooperation to emerge and persist, such as reciprocity, reputation, or
204 shared norms, is essential for building robust and socially aligned autonomous systems.

205 3.4 Simple Markov games as social dilemmas

206 This work focuses on a class of simple Markov games involving social dilemmas. These games are
207 *simple* in the sense that they contain a small number of states, typically one or two, and a limited
208 action set per agent, often consisting of two or three possible actions. Crucially, these games
209 involve repeated interactions rather than single-shot encounters: agents interact over multiple
210 time steps, which allows for the emergence of complex, adaptive strategies. Moreover, while we
211 call these games *simple* the space of behaviors which they can model is far from simple. The
212 dynamics of which are still not well understood in the literature.

213 Compared to the complex Markov games typically studied in MARL, simple games offer a
214 distilled view of the core strategic tensions that define real-world social dilemmas. By abstract-
215 ing away domain-specific mechanics and environmental intricacies, these minimal environments
216 help avoid conclusions that are overly dependent on the quirks of particular settings. This mir-
217 rors the problem of overfitting in machine learning, where models may learn *shortcuts* and exploit
218 spurious correlations, such as associating grass with the label "dog," instead of learning robust,
219 generalizable patterns. Similarly, agents trained in complex environments can develop brittle
220 strategies that exploit incidental features of the environment rather than learning the underlying
221 strategic structure.

222 Simple Markov games mitigate the risk of overfitting to environmental intricacies by isolat-
223 ing the core social dilemma itself. This isolation allows for theoretical insights that generalize

224 more reliably across different domains. Additionally, the simplicity of these games enables exact
225 computation of rewards and learning gradients, enhancing interpretability and providing a high
226 degree of analytical tractability. Consequently, these environments serve as powerful tools for
227 studying the dynamics of learning, adaptation, and strategic behavior in multi-agent systems.

228 The following sections describe specific social dilemmas studied, demonstrating the rich
229 range of cooperative and competitive dynamics possible in repeated simple Markov games.

230 **Prisoner’s dilemma (PD):** The prisoner’s dilemma is a canonical social dilemma, modeled here as
231 a repeated game with a single state and two possible actions: cooperate (C) or defect (D). In each
232 round, both agents simultaneously select their actions without knowledge of the other’s current
233 choice. The resulting pair of actions determines their individual rewards, which are defined by
234 a payoff matrix characterized by four key parameters: the reward for mutual cooperation (R),
235 the punishment for mutual defection (P), the temptation payoff for unilateral defection (T), and
236 the sucker’s payoff for unilateral cooperation (S). A commonly employed parameterization is
237 $(R, S, T, P) = (3, 0, 5, 1)$, which encapsulates the strategic tension central to the dilemma.

238 Defection strictly dominates cooperation for the individual, meaning that regardless of the
239 other agent’s action, choosing to defect yields a higher immediate reward. For example, if the
240 other agent cooperates, defecting yields the temptation reward $T = 5$ rather than the mutual
241 cooperation reward $R = 3$. If the other defects, defecting yields $P = 1$ instead of the sucker’s
242 reward $S = 0$. Despite this incentive to defect, mutual cooperation results in a collectively better
243 outcome, with each agent receiving $R = 3$ compared to $P = 1$ in mutual defection. This creates
244 a tension between self-interest and the common good: while defection is individually rational, it
245 leads to worse outcomes for both agents when both defect.

246 In the repeated prisoner’s dilemma, also known as the iterated prisoner’s dilemma (IPD),
247 these interactions occur over multiple time steps, allowing agents to adapt their behavior based
248 on previous rounds. This repeated structure enables the development of complex strategies
249 such as reciprocity, punishment, and forgiveness, which can sustain cooperation despite the
250 temptation to defect in any single round. By conditioning actions on past behavior, agents can
251 build trust and enforce social norms, making the repeated prisoner’s dilemma a fundamental
252 framework for studying how cooperation can emerge and be maintained in multi-agent systems
253 facing conflicting incentives.

254 **Two-state coin game:** The original coin game, introduced by Lerer and Peysakhovich [31], is a
255 spatially structured multi-agent Markov game designed to capture the complexities of cooperation
256 and competition in dynamic, spatially extended environments. In this setup, two agents
257 occupy a grid world where red and blue coins appear randomly at different locations. Each
258 agent is assigned a color, red or blue, and receives positive rewards for collecting coins of any
259 color. Critically, when an agent collects a coin of the opponent’s color, it also imposes a penalty
260 on the other player. This setup captures a social dilemma with a spatial component: agents must
261 balance immediate self-interest against the longer-term consequences of their actions in a shared
262 space.

263 The two-state coin game removes all the “non-rewarding” states from the original environment.
264 In this simplified version, each state corresponds solely to whether the coin present is
265 red or blue, and the rewards match those of the original game when each agent is positioned
266 immediately adjacent to the coin. By eliminating sparse, non-informative states, the two-state
267 coin game offers improved learning efficiency and yields results that are easier to interpret.

268 Studying this two-state coin game is vital for understanding learning dynamics in spatially
269 extended social dilemmas, as many real-world social interactions unfold in spatially structured
270 settings, ranging from competition over natural resources in ecological systems to coordination
271 among autonomous vehicles in traffic networks. Examining algorithms within this streamlined
272 yet spatially meaningful framework provides valuable insights into how spatial factors influence
273 learning, strategy development, and the delicate balance between cooperative and competitive
274 behaviors. Such insights are critical for designing resilient multi-agent systems capable of navi-
275 gating and resolving complex spatial social dilemmas.

276 **Nonlinear donation game:** The donation game is a classical model for studying altruism and
277 cooperation. In its original form, each agent may choose to incur a cost c to provide a benefit
278 b to another agent. traditionally, the donation game assumes a linear relationship between the
279 cost incurred and the benefit conferred. That is, cooperation always improves group welfare,
280 and more cooperation is always better. However, this assumption fails to capture a range of real-
281 world situations in which increasing levels of cooperation may produce diminishing rewards,
282 or even net harm. For example, in public health, a moderate level of social distancing might
283 effectively reduce disease spread with tolerable inconvenience, whereas extreme isolation may
284 impose excessive social and economic costs that outweigh the additional benefits.

285 To model this non-linearity, the nonlinear donation game introduces a richer action space and
286 a more nuanced reward structure. Instead of two actions (cooperate or defect), each agent now
287 has three: one defection action (D) and two levels of cooperation (c_1 and c_2). These represent
288 increasing degrees of altruistic behavior. Specifically, c_1 incurs a smaller cost and delivers a
289 smaller benefit b_1 , while c_2 incurs a larger cost and delivers a larger benefit b_2 , with $c_2 > c_1 > 0$
290 and $b_2 > b_1 > 0$. Importantly, the game is constructed so that the net social value (i.e., total
291 benefit minus total cost) is maximized not at the highest cooperation level, but at the moderate
292 one: $b_1 - c_1 > b_2 - c_2 > 0$.

293 This non-linearity introduces a fundamentally different strategic challenge. Unlike in the
294 prisoner's dilemma, where increasing cooperation is unambiguously better for the group, here
295 the socially optimal outcome occurs at an intermediate level of cooperation. Full cooperation may
296 be too costly to justify the additional benefits, while no cooperation leaves significant potential
297 gains unrealized. As a result, the game poses a subtler learning problem: agents must not only
298 learn to cooperate but also learn how much to cooperate. As such, the nonlinear donation game
299 provides a compelling testbed for understanding whether learning algorithms merely default to
300 maximal cooperation or are capable of discovering socially optimal behaviors.

301 **Ecological prisoner's dilemma:** This game extends the classic prisoner's dilemma by adding
302 an additional state to introduce ecological feedback. The first state mirrors the standard setup,
303 in which agents face the familiar tension between short-term self-interest and long-term group
304 benefit. However, repeated mutual defection in this state leads to a transition into a second state
305 that represents environmental degradation, characterized by uniformly negative rewards for all
306 joint actions. This models the long-term consequences of over-exploitation, such as resource
307 depletion, pollution, or ecological collapse.

308 The key innovation in this variant is the coupling of agent behavior with environmental dy-
309 namics: the agents' collective actions directly influence the transition between states, embedding
310 the strategic dilemma within a broader ecological context. Unlike in the standard prisoner's
311 dilemma, where the incentive to defect dominates, the looming threat of environmental collapse

312 introduces a natural incentive to maintain cooperation as a preventive measure. This shift re-
313 frames the problem as not just a question of whether agents will cooperate, but whether they can
314 internalize the long-term consequences of their actions through learning.

315 Studying this ecological variant is important for several reasons. First, it provides a principled
316 way to investigate how learning agents respond when the rewards are endogenous and evolve
317 as a function of behavior, rather than being fixed. Second, it sheds light on whether cooperation
318 can be sustained in the face of long-term collective risk. By comparing agent behavior in this
319 setting to that observed in the classic prisoner’s dilemma, we can examine whether the presence
320 of a natural incentive to cooperate leads to qualitatively different learning dynamics or long-term
321 equilibria. This has direct relevance to real-world challenges in climate strategy, sustainability,
322 and commons governance, where ecological feedback loops are both powerful and pervasive.

323 3.5 Adaptation and learning

324 To analyze the emergence of cooperation in social dilemmas, a population of N agents is con-
325 sidered, engaging in repeated pairwise interactions. Agents adopt stochastic strategies that are
326 selfishly updated via gradient ascent, facilitating the study of strategy dynamics under decen-
327 tralized learning in a range of environments.

328 **Strategy representations.** Strategies are represented as *memory-one strategies* which condition
329 behavior solely on the outcome of the previous round of interaction. Formally, let \mathcal{A} denote the
330 set of possible actions. Since each agent observes both their own and their opponent’s action
331 from the previous round, there are $|\mathcal{A}|^2$ possible joint actions to condition on. A memory-one
332 strategy defines, for each such joint action pair $(a_i^{t-1}, a_j^{t-1}) \in \mathcal{A} \times \mathcal{A}$, a probability distribution
333 over next actions:

$$\pi(a_i^t | a_i^{t-1}, a_j^{t-1}) \in \Delta(\mathcal{A}), \quad (4)$$

334 where $\Delta(\mathcal{A})$ is the probability simplex over actions and t is the round of play. While memory-one
335 strategies abstract away the full history of play, they do not limit the expressiveness of the strategy
336 space: any strategy that can be represented as a full memory can also be represented using
337 a memory-one strategy. Moreover, restricting attention to memory-one strategies significantly
338 reduces the size of the state space, thereby enhancing both learning efficiency and interpretability.

339 We consider two types of strategy parameterizations for implementing memory-one strate-
340 gies: tabular strategies and neural network strategies.

341 *Tabular strategies* represent the strategy explicitly as a lookup table over the $|\mathcal{A}|^2$ previous
342 joint action pairs. Each entry in the table specifies a distribution over the agent’s next action.
343 This discrete and fully specified structure makes tabular strategies highly interpretable. Their
344 interpretability makes them ideally suited for analyzing behavioral dynamics in simple, well-
345 controlled environments. However, tabular strategies scale poorly as the action space grows or
346 when the environment includes richer state information. Their use is thus limited to environ-
347 ments with small, discrete input spaces.

348 *Neural network strategies* offer a more scalable alternative. In our framework, they are still
349 memory-one in structure: the network takes as input a representation of the previous joint action

350 (a_i^{t-1}, a_j^{t-1}) , encoded for instance as a one-hot vector, and outputs a distribution over actions:

$$\pi_\theta(a_i^t | a_i^{t-1}, a_j^{t-1}) = \text{softmax}(f_\theta(a_i^{t-1}, a_j^{t-1})), \quad (5)$$

351 where f_θ is a neural network with parameters θ . Neural strategies are capable of generalizing
 352 across input patterns and can scale to environments with large or continuous observation spaces.
 353 However, this expressiveness comes at a cost: the function learned by the network is not easily
 354 interpretable, and small changes in parameters can induce correlated, global changes in behavior.
 355 This makes it difficult to attribute specific actions or outcomes to identifiable behavioral rules.

356 **Gradient-based strategy updates.** Agents use gradient based learning rules to update their
 357 strategies selfishly. That is, they ignore the reward of their opponent and seek only to maximize
 358 their own long-term expected reward. Let π_i and π_j denote the strategies used by agents i and j ,
 359 respectively. The quality of strategy π_i when facing π_j is quantified by the expected discounted
 360 reward:

$$U(\pi_i, \pi_j) = \mathbb{E}_{\tau \sim (\pi_i, \pi_j)} \left[\sum_{t=0}^{\infty} \gamma^t r_i^t \right], \quad (6)$$

361 where τ is a trajectory induced by the joint strategies, r_i^t is the reward received by agent i at time
 362 t , and $\gamma \in (0, 1)$ is the discount factor. The gradient ascent update rule modifies strategies in the
 363 direction of the maximal gradient:

$$\pi_i^{t+1} = \pi_i^t + \eta \nabla_{\pi_i^t} U(\pi_i^t, \pi_j^t), \quad (1)$$

364 where η is the learning rate. These updates are local and selfish: each agent optimizes its own
 365 reward without considering the broader population dynamics.

366 In simple Markov games $\nabla_{\pi_i} U(\pi_i, \pi_j)$ can be computed explicitly. In complex environments
 367 where exact gradients are intractable, agents estimate $\nabla_{\pi_i} U(\pi_i, \pi_j)$ using *policy gradient methods*.
 368 These approaches optimize a parameterized policy, $\pi : S \rightarrow \Delta(A_i)$ by maximizing the expected
 369 return,

$$U(\theta) = \mathbb{E}_{\tau \sim \pi_\theta} \left[\sum_{t=0}^{\infty} \gamma^t r^t \right]. \quad (7)$$

370 Using the log-derivative trick, the gradient can be expressed as:

$$\nabla_\theta U(\theta) = \mathbb{E}_\tau \left[\sum_{t=0}^{\infty} \nabla_\theta \log \pi_\theta(a_t | s_t) \cdot R_t \right], \quad (8)$$

371 where $R_t = \sum_{k=t}^{\infty} \gamma^{k-t} r^k$ is the return from time t . This formulation allows the use of sampled
 372 episodes to estimate gradients, enabling learning in environments where explicit models are
 373 unavailable. The behavior of selfish agents in social dilemmas is studied using both exact and
 374 policy gradients.

375 **Population-level learning dynamics.** This study investigates the impact of population stochasticity in social dilemmas through a framework where a population of N agents repeatedly participates in decentralized, pairwise interactions governed by the learning rules described above. The learning process unfolds over many rounds of interaction. In each round, the population is partitioned into $N/2$ pairs. Each pair plays a repeated Markov game using their current strategies at time t . For a given interaction between agent i and agent j , the outcome is evaluated using the expected discounted reward $U(\pi_i, \pi_j)$. Agent j receives a reward $U(\pi_j, \pi_i)$. These rewards are used to update each agent's policy using the gradient-based learning rules described in previous sections.

384 After the policies are updated, the population is re-paired for the next round of interaction. 385 We consider two distinct pairing mechanisms, which represent qualitatively different interaction 386 structures:

- 387 • **Fixed Pairings:** Each agent is paired with the same partner across all rounds. This regime 388 corresponds to standard “naive self-play,” where agents co-adapt in isolation.
- 389 • **Random Pairings:** Agent pairings are assigned randomly after each round. This simulates 390 a well-mixed population in which agents interact with a broad and changing set of partners 391 over time. Random pairing introduces population-level stochasticity and exposes agents to 392 a greater variety of strategies, potentially enabling more robust and generalizable forms of 393 cooperation.

394 A visual summary of this learning and adaptation process is provided in ?? . This population- 395 based learning framework enables a systematic exploration of how the structure of social inter- 396 action influences the trajectory of behavioral evolution. In particular, it offers insight into how 397 diverse encounters and patterns of social exposure affect the resolution of social dilemmas, in- 398 cluding the emergence and stability of cooperation in the absence of coordination or centralized 399 control.

400 4 Strategy Initialization

401 The way strategies are initialized in population-based learning sets the stage for how agents 402 explore and grow through interaction. When agents begin with a broad range of strategies, 403 they experience a richer variety of behaviors, leading to more effective learning. However, if the 404 initialization is too narrow, agents become confined to a small set of behaviors, which limits the 405 benefits of population-based learning and can make it no better than naive self-play.

406 It is important to understand that diversity in the parameter space alone does not guarantee 407 meaningful diversity in behavior. Parameter space diversity refers to variation in the underlying 408 numerical parameters that specify a strategy. For example, in neural network strategies, this cor- 409 responds to differences in the network weights; in tabular strategies, this means different proba- 410 bility values assigned to actions. While parameter diversity measures how “far apart” strategies 411 are in terms of their internal representation, it does not necessarily reflect how differently those 412 strategies behave in practice.

413 In contrast, behavior space diversity is concerned with the variation in the observable con- 414 sequences of deploying a strategy. In multi-agent settings, this means how a strategy's actions 415 influence the rewards it obtains when interacting with other agents. Formally, we define the

⁴¹⁶ behavior of a strategy π_i with respect to a population \mathcal{P} as the expected reward achieved when
⁴¹⁷ interacting with strategies sampled from \mathcal{P} :

$$V_{\text{avg}}(\pi_i, \mathcal{P}) = \mathbb{E}_{\pi_j \sim \mathcal{P}} [U(\pi_i, \pi_j)]. \quad (9)$$

⁴¹⁸ This definition grounds behavior in the functional impact of a strategy within its interaction
⁴¹⁹ context, rather than its internal parameterization.

⁴²⁰ This distinction is crucial because many environments exhibit nonlinear reward dynamics,
⁴²¹ where uniform sampling of the parameter space often does *not* produce a uniform or meaningful
⁴²² coverage of behavioral space. Small parameter changes may correspond to large behavioral
⁴²³ differences or none at all. Conversely, in linear reward environments, parameter variation more
⁴²⁴ directly translates to variation in behavior and payoffs.

⁴²⁵ To demonstrate the influence of strategy initialization on parameter diversity and behavior,
⁴²⁶ two complementary approaches based on autoencoders are developed: one that captures vari-
⁴²⁷ ation in strategy parameters, and another specifically designed to capture behavioral variation
⁴²⁸ through reward outcomes.

⁴²⁹ 4.1 Parameter space autoencoder

⁴³⁰ The parameter space autoencoder, shown in Figure 1a, is trained to compress and reconstruct
⁴³¹ high-dimensional strategy representations, optimizing for minimal reconstruction loss. Given a
⁴³² strategy π , the encoder E maps it to a low-dimensional latent vector $z = E(\pi)$, and the decoder
⁴³³ D attempts to reconstruct π from z , such that the reconstruction loss

$$\mathcal{L}_{\text{rec}} = \|\pi - D(E(\pi))\|^2 \quad (10)$$

⁴³⁴ is minimized.

⁴³⁵ This setup ensures that the latent space captures the structure of the parameter space and
⁴³⁶ clusters similar parameters together. Note, however, that it is agnostic to the actual behavior
⁴³⁷ of strategies. Two strategies that differ significantly in parameter space may lead to indistin-
⁴³⁸ guishable in-game behavior. Moreover, the parameter space autoencoder only helps visualize
⁴³⁹ parameter space diversity of strategies and does not capture meaningful behavioral distinctions.

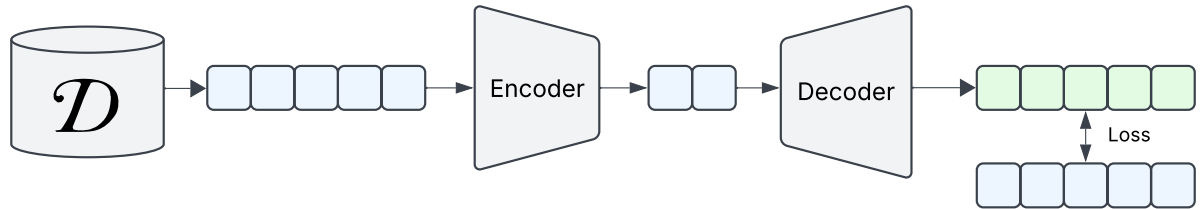
⁴⁴⁰ 4.2 Behavior space autoencoder

⁴⁴¹ To specifically capture agent behavioral, a behavior space autoencoder is introduced. This model
⁴⁴² takes pairs of strategies (π_i, π_j) as input and learns to predict their long-term expected rewards,
⁴⁴³ denoted $U(\pi_i, \pi_j)$.

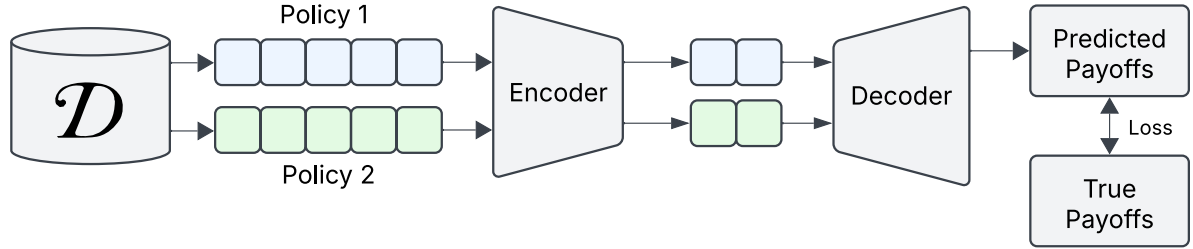
⁴⁴⁴ The behavior space autoencoder consists of an encoder E that maps each strategy to a latent
⁴⁴⁵ representation $z_i = E(\pi_i)$ and $z_j = E(\pi_j)$. The decoder then takes (z_i, z_j) as input and outputs
⁴⁴⁶ the predicted rewards to each player when these strategies interact. The loss function $\mathcal{L}_{\text{payoff}}$ is
⁴⁴⁷ defined as:

$$\mathcal{L}_{\text{reward}} = |U(\pi_i, \pi_j) - \hat{U}(E(\pi_i), E(\pi_j))|^2. \quad (11)$$

⁴⁴⁸ This architecture enforces a crucial inductive bias: strategies that produce similar outcomes
⁴⁴⁹ in terms of interaction rewards are embedded nearby in the latent space, even if their param-
⁴⁵⁰ eterizations differ drastically. In this way, the behavior space autoencoder captures behavioral
⁴⁵¹ equivalence or similarity and emphasizes diversity in terms of strategic effect rather than raw
⁴⁵² structure, as shown in Figure 1b.



(a) Parameter space autoencoder. This autoencoder is trained to minimize reconstruction loss between the original and decoded strategies, compressing strategies purely based on their raw parameter vectors. As a result, the latent space clusters strategies with similar parameterizations, regardless of how they behave during interactions.



(b) Behavior space autoencoder. In contrast to the parameter space autoencoder, this model embeds strategies based on how they interact in the environment. It takes pairs of strategies and predicts their expected rewards, learning a latent space where strategies with similar behavior and reward profiles are placed nearby. This behavior-aware representation captures the strategic equivalence and diversity that arise from actual gameplay outcomes, even if the underlying parameterizations differ widely.

Figure 1: Autoencoder Architectures for Strategy Embedding. These diagrams illustrate two distinct approaches to creating strategy embeddings. The parameter space autoencoder (a) focuses on compressing raw parameter vectors, while the behavior space autoencoder (b) emphasizes strategic behavior as inferred from expected interaction payoffs. Together, these models enable both structural and functional interpretations of the strategy landscape.

453 **4.3 Visualizing parameter and behavioral diversity**

454 To understand the impact of strategy initialization, two initialization schemes are analyzed us-
455 ing both a pre-trained *parameter space autoencoder* and a pre-trained *behavior space autoencoder*,
456 which embed memory-one strategies for the prisoner’s dilemma into a two-dimensional space.
457 These embeddings facilitate interpretation of both parameter variation and behavioral diversity
458 as reflected in the reward structure.

459 We consider two initialization schemes:

460 • **Dirichlet (1.0):** Equivalent to uniform sampling over the simplex.
461 • **Dirichlet (0.1):** Favors sparse strategies with probability mass near the corners [0, 1].

462 A total of 100,000 strategies are sampled from each distribution and processed through the
463 respective encoders. The resulting embeddings are visualized in Figure 2.

464 Figure 2a and Figure 2c show the embeddings produced by the traditional autoencoder. When
465 sampling from Dirichlet (1.0), the strategies appear broadly distributed in parameter space, sug-
466 gesting high surface-level diversity. In contrast, Dirichlet (0.1) generates tighter clusters in pa-
467 rameter space, implying that the sampled strategies seem more similar in terms of their raw
468 parameters.

469 However, a contrasting picture emerges when the embeddings are examined from the per-
470 spective of actual strategic behavior. Figure 2b and Figure 2d present embeddings derived from
471 the BSAE, corresponding to strategies sampled from Dirichlet (1.0) and Dirichlet (0.1), respec-
472 tively. Notably, Figure 2d reveals that strategies sampled from Dirichlet (0.1) span a wide and
473 comprehensive region of behavior space, including its extreme edges. This is significant, as it
474 highlights the presence of diverse and extreme strategic profiles within the prisoner’s dilemma
475 behavior space.

476 Efficient coverage of this behavior space is critical because incorporating these behavioral
477 extremes allows agents to learn from the broadest possible range of strategies. When initialized
478 in this manner, agents can interpolate between a more extensive set of strategies, overcoming the
479 limitations imposed by their initial parameterization. In contrast, Figure 2b shows that, despite
480 the apparent parameter-level diversity produced by Dirichlet (1.0), many behavioral extremes
481 remain unexplored. Even with 100,000 sampled strategies, certain crucial regions of the behavior
482 space are left uncovered, potentially restricting an agent’s ability to learn from key strategic
483 profiles during training.

484 This distinction is crucial: diversity in parameter space does not necessarily equate to di-
485 versity in behavior space. While Dirichlet (1.0) spreads samples broadly across the pa-
486 rameter simplex, it does not fully cover the behavioral landscape and therefore misses high-impact
487 strategies located at the edges of the behavior spectrum. Conversely, strategies sampled from
488 Dirichlet (0.1), despite exhibiting less apparent diversity in parameter space, actually achieve
489 broad and comprehensive coverage of behavior space. Thus, sampling from a Dirichlet prior with
490 a low concentration parameter offers a powerful mechanism for initializing strategies that ensure
491 rich behavioral diversity, enabling more effective exploration and learning within population-
492 based frameworks.

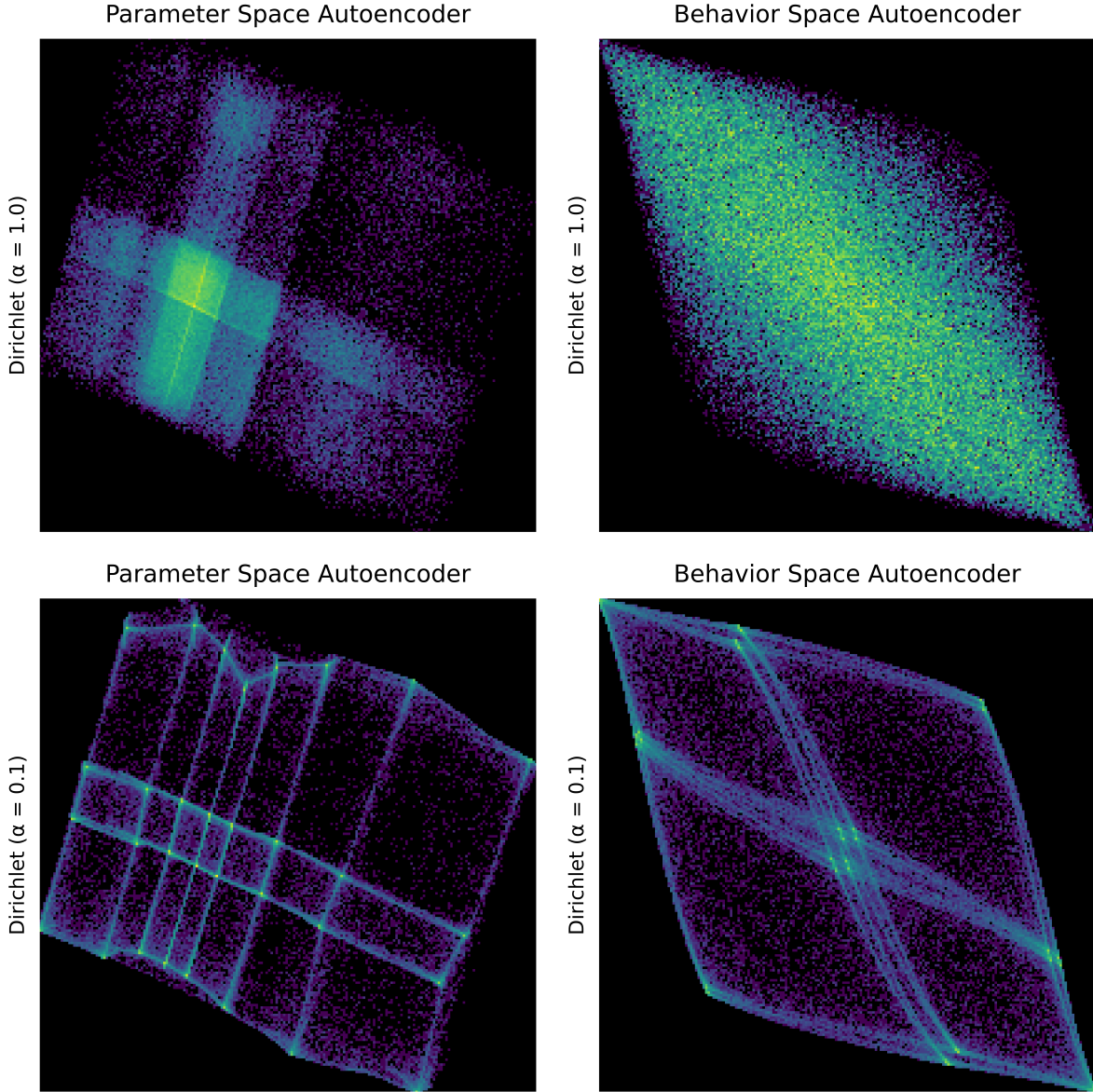


Figure 2: Visualization of 100,000 sampled strategies from two Dirichlet distributions, embedded using a traditional autoencoder (Figures a and b) and a payoff-based autoencoder (Figures c and d). **(a)** Dirichlet (1.0) with parameter space autoencoder shows widespread coverage in parameter space. **(b)** Dirichlet (1.0) with behavior space autoencoder fails to capture the extremes (corners) of the behavior distribution. **(c)** Dirichlet (0.1) with parameter space autoencoder shows tighter parameter clusters. **(d)** Dirichlet (0.1) with behavior space autoencoder reveals broad behavioral coverage, particularly at the extremes of the strategy space. These results illustrate that parameter diversity does not necessarily translate to behavioral diversity and motivate the use of sparse Dirichlet priors to ensure exposure to qualitatively distinct strategic behaviors.

493 **5 Experiments**

494 **5.1 Implementation details**

495 The proposed population learning framework was evaluated across the four social dilemmas
496 defined in Section 3.2. These games differ in their action spaces and payoff structures, and
497 involve repeated interactions. After each round, agents updated their strategies using either
498 exact or approximate policy gradients.

499 In the exact gradient setting, long-term expected rewards were computed precisely using
500 full knowledge of the environment dynamics or exact value computation. This allowed for a
501 higher learning rate of 0.1, as the precise gradient information reduced the risk of destabilizing
502 updates. In contrast, approximate gradients were computed using vanilla policy gradient with
503 rollouts of 250 time steps. Due to the increased variance in these estimates, a smaller learning
504 rate of 0.05 was used to ensure stability. All updates were performed using stochastic gradient
505 descent (SGD), which is better suited for non-stationary multi-agent environments. SGD provides
506 more stable dynamics compared to adaptive optimizers like Adam, which may overfit to rapidly
507 changing local gradients.

508 Both tabular and neural network (NN) strategies were implemented. In the tabular setting,
509 strategies were stored as explicit state-action mappings, with each value updated independently.
510 For neural strategies, each was represented by a feedforward neural network with a single hidden
511 layer. The hidden layer had a width equal to four times the size of the state-space. Initial
512 strategies were sampled independently for each agent using a Dirichlet distribution over the
513 action simplex. This initialization method enabled controlled exploration of initial diversity.

514 Performance was assessed using the average total population reward. This metric serves as
515 a meaningful proxy for social efficiency and cooperation: higher average rewards indicate not
516 only successful individual behavior but also emergent alignment among agents. Importantly, this
517 metric captures more than just full cooperation, especially in games where blindly maximizing
518 cooperation can be suboptimal, making it a robust measure of overall population-level effective-
519 ness. The learning framework was evaluated against a baseline of naïve self-play, in which agents
520 interact with fixed opponents that do not change after each round. All results are reported as
521 averages over 10 random seeds.

522 **5.2 Exact gradients**

523 Figure 3 summarizes the learning dynamics of populations of size $N = 50$, trained using exact
524 gradient updates and tabular strategies, across several distinct Markov games. Each row in the
525 figure corresponds to a different social dilemma, while the two columns compare two experi-
526 mental conditions: (1) fixed pairings, where agents are matched with the same partner across
527 rounds of the repeated game, and (2) random pairings, where partners are reshuffled after each
528 round. The y-axis reports the average population reward over time (x-axis), serving as a proxy
529 for the overall social welfare.

530 Across all games, a consistent and robust pattern emerges: random pairings systematically
531 outperform fixed pairings in terms of long-run average population reward. This result is particu-
532 larly striking because it holds across a diverse set of social dilemmas, each with its own strategic
533 structure and payoff landscape. The presence of partner randomization significantly improves

534 learning outcomes, enabling agents to escape from local equilibria associated with mutual defec-
535 tion and to discover globally superior strategies.

536 In the standard repeated prisoner’s dilemma, agents paired with the same partner learn
537 to defect almost immediately. This behavior leads to low and stagnant population rewards.
538 In contrast, when partners are randomized after each round, agents initially follow a similar
539 trajectory toward defection, but then exhibit a strong and sustained reversal. Over time, the
540 population converges toward strategies that support cooperation, leading to a markedly higher
541 average reward. This rebound suggests that exposure to a broader variety of partner strategies
542 encourages the evolution of more generalizable, cooperative strategies.

543 Similar trends are observed in the coin game and the nonlinear donation game. Under fixed
544 pairings, agents again fall into early defection traps, never recovering to cooperative norms.
545 However, random pairings lead to recovery and eventual convergence toward higher-reward
546 outcomes. The nonlinear donation game is particularly illustrative, as it features a non-monotonic
547 relationship between cooperation and global welfare. Unlike simpler dilemmas where maximum
548 cooperation aligns with the global optimum, here it is an intermediate level of cooperation that
549 yields the highest population reward. Remarkably, the population with randomized partners
550 does not merely maximize cooperation blindly; rather, it converges to this more nuanced global
551 optimum. This finding underscores the capacity of diverse interactions to enable agents to learn
552 not just pro-social behavior, but strategically optimal cooperation.

553 The ecological variant of the prisoner’s dilemma introduces a modified incentive structure
554 in which cooperation is more naturally rewarded. In this case, both fixed and random pairings
555 result in an increase in cooperative behavior. Agents in fixed pairs gradually learn to cooperate
556 roughly two-thirds of the time, resulting in an average population reward just above -1 , a
557 significant improvement over the mutual defection outcome of -5 . Nevertheless, even in this
558 more favorable environment, fixed pairs plateau below the optimal outcome. In contrast, ran-
559 dom pairings drive the population to full cooperation, achieving the global maximum. This
560 again highlights the role of interaction diversity in promoting socially efficient outcomes, even in
561 games where cooperation is already partially incentivized.

562 Overall, these findings demonstrate that the structure of partner interaction significantly
563 shapes the emergent strategies in multi-agent learning. Fixed pairings promote myopic, partner-
564 specific strategies that are prone to early convergence on suboptimal equilibria. In contrast,
565 randomization introduces variability and strategic uncertainty, which serves as a form of reg-
566 ularization or exploration, driving the system toward more generalizable and socially optimal
567 solutions.

568 These results connect between MARL and foundational insights from evolutionary game
569 theory, where mechanisms that promote social mixing are known to support the emergence
570 of cooperation. Our findings provide both algorithmic and empirical reinforcement of these
571 theoretical principles in the context of modern learning agents. By showing that randomized
572 partner interactions consistently lead to more favorable collective outcomes, this work bridges
573 the gap between evolutionary models of cooperation and contemporary MARL frameworks.
574 From a design standpoint, the results suggest that artificial systems composed of interacting
575 agents should incorporate dynamic and heterogeneous partner interactions to avoid pathological
576 convergence to selfish or suboptimal equilibria. Partner randomization and structural diversity
577 act as an implicit curriculum, encouraging broader exploration and generalization.

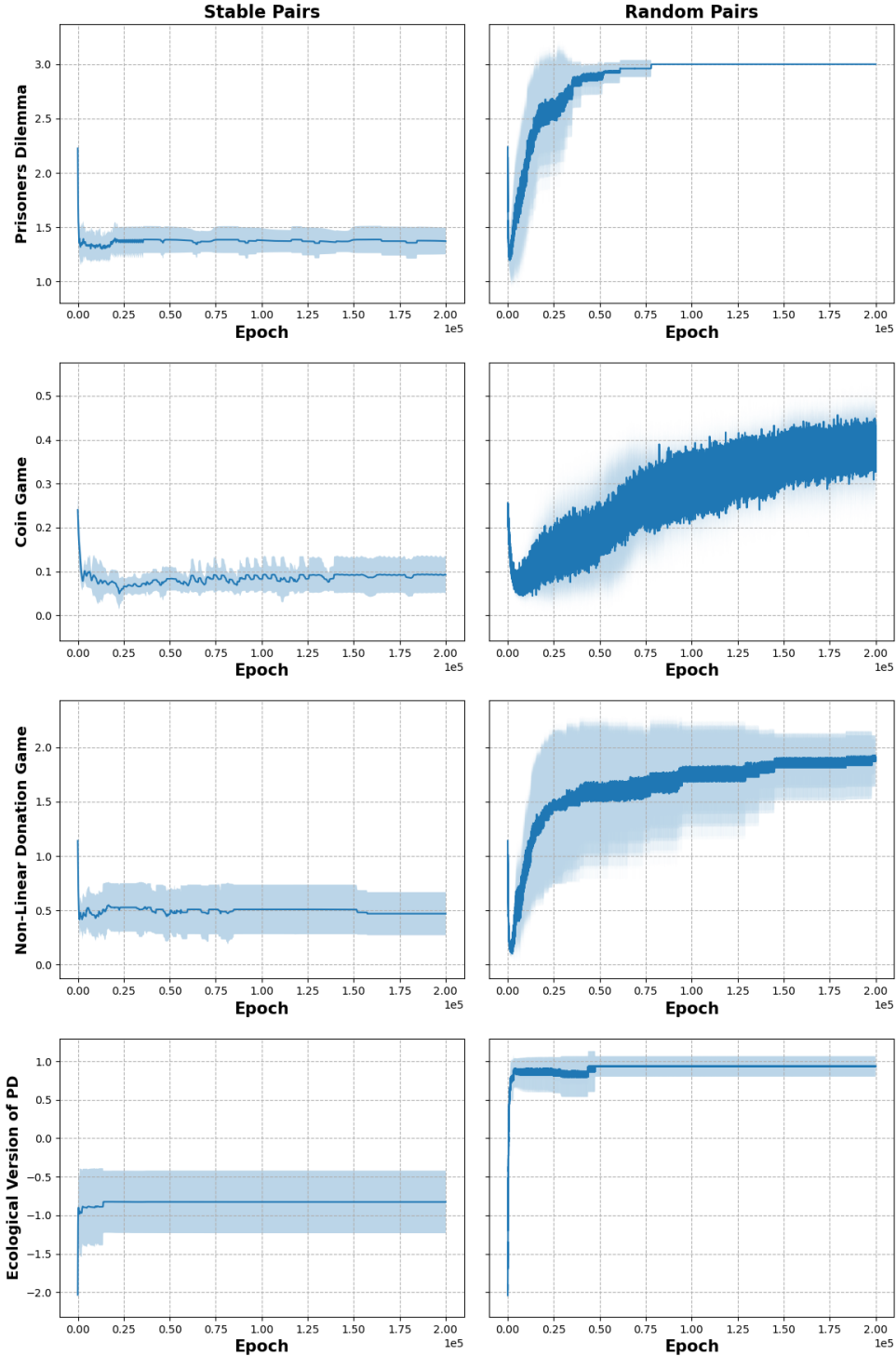


Figure 3: Impact of Interaction Stochasticity with Exact Gradients. A population of 50 agents with tabular, parameterized strategies was initialized using a Dirichlet (0.75, 0.75) distribution. We compare the performance of stable pairings, where opponents remain fixed, with random pairings, where opponents are randomized each round. This figure demonstrates that fixed interactions often lead to a rapid convergence to a suboptimal equilibrium, while stochastic interactions, characterized by randomly changing opponents, can reverse these tendencies.

578 **5.3 Approximate gradients**

579 While the previous section examined learning dynamics under exact gradient updates, such
580 methods are rarely practical due to their reliance on complete knowledge of the environment
581 dynamics and reward functions. To address this limitation, we now consider agents that learn
582 via approximate gradient methods, focusing on policy gradient algorithms [32].

583 Figure 4 presents the average population reward over time for a population of size $N = 50$
584 trained with policy gradient updates using tabular strategy representations. As in the exact
585 gradient setting, each row corresponds to a different social dilemma and the columns compare
586 learning under fixed and random pairings.

587 Despite the noise introduced by policy gradient estimation, we observe a surprisingly con-
588 sistent replication of the dynamics observed under exact gradients, albeit over a longer learning
589 horizon. In all games studied, populations with random pairings consistently achieve higher
590 long-term rewards than those with fixed partners. Agents with fixed partners tend to converge
591 toward low-reward equilibria, characterized by mutual defection or locally optimal but globally
592 suboptimal cooperative strategies. In contrast, randomized interactions allow agents to escape
593 these traps and discover globally optimal strategy profiles.

594 While policy gradients yield an unbiased estimate of the exact gradient, the replication of
595 cooperative dynamics in this setting is non-trivial. In multi-agent environments, the learning
596 landscape is inherently non-stationary: each agent’s strategy update alters the environment ob-
597 served by others. Under these conditions, local gradient estimation errors can accumulate and
598 interact in complex ways, leading to drastically different strategy pairings and optimization tra-
599 jectories. Such instabilities could, in principle, derail the previous findings entirely. The fact
600 that partner randomization still leads to cooperative behavior, even under these noisy conditions,
601 demonstrates that randomized interactions create a *powerful signal* encouraging independent self-
602 ish agents to cooperate. And this powerful signal survives even under noisy updates and more
603 realistic environmental conditions.

604 **5.4 NN parameterization**

605 Tabular strategies offer a high degree of interpretability: each parameter directly corresponds to
606 an action probability, allowing for transparent analysis of population dynamics and behavioral
607 diversity. NNs, by contrast, introduce an abstract parameterization that enables scalability to
608 high-dimensional and complex state spaces, which is critical for many real-world MARL prob-
609 lems, but at the cost of reduced interpretability and increased training complexity.

610 In the *tabular setting*, strategies are initialized by sampling directly from a Dirichlet distribu-
611 tion over the action simplex. This allows for fine control over initial diversity: lower concentration
612 parameters yield more extreme (sparse) distributions, while higher values produce more uniform
613 mixtures. In the *NN setting*, we pre-train each network to match a tabular policy sampled from
614 the same Dirichlet distribution, ensuring that the initial output policy distribution (rather than
615 the network weights) conforms to the same statistical structure.

616 Despite exhibiting similar behavior at initialization, neural networks (NNs) are substan-
617 tially more sensitive to the concentration of the Dirichlet prior. Figure 5 illustrates this effect
618 in the repeated prisoner’s dilemma under random pairings. Populations initialized with low-
619 concentration priors (e.g., Dirichlet (0.5, 0.5)) reliably recover cooperative behavior in populations
620 of size 50. In contrast, populations initialized with more uniform priors (e.g., Dirichlet (1.0, 1.0))

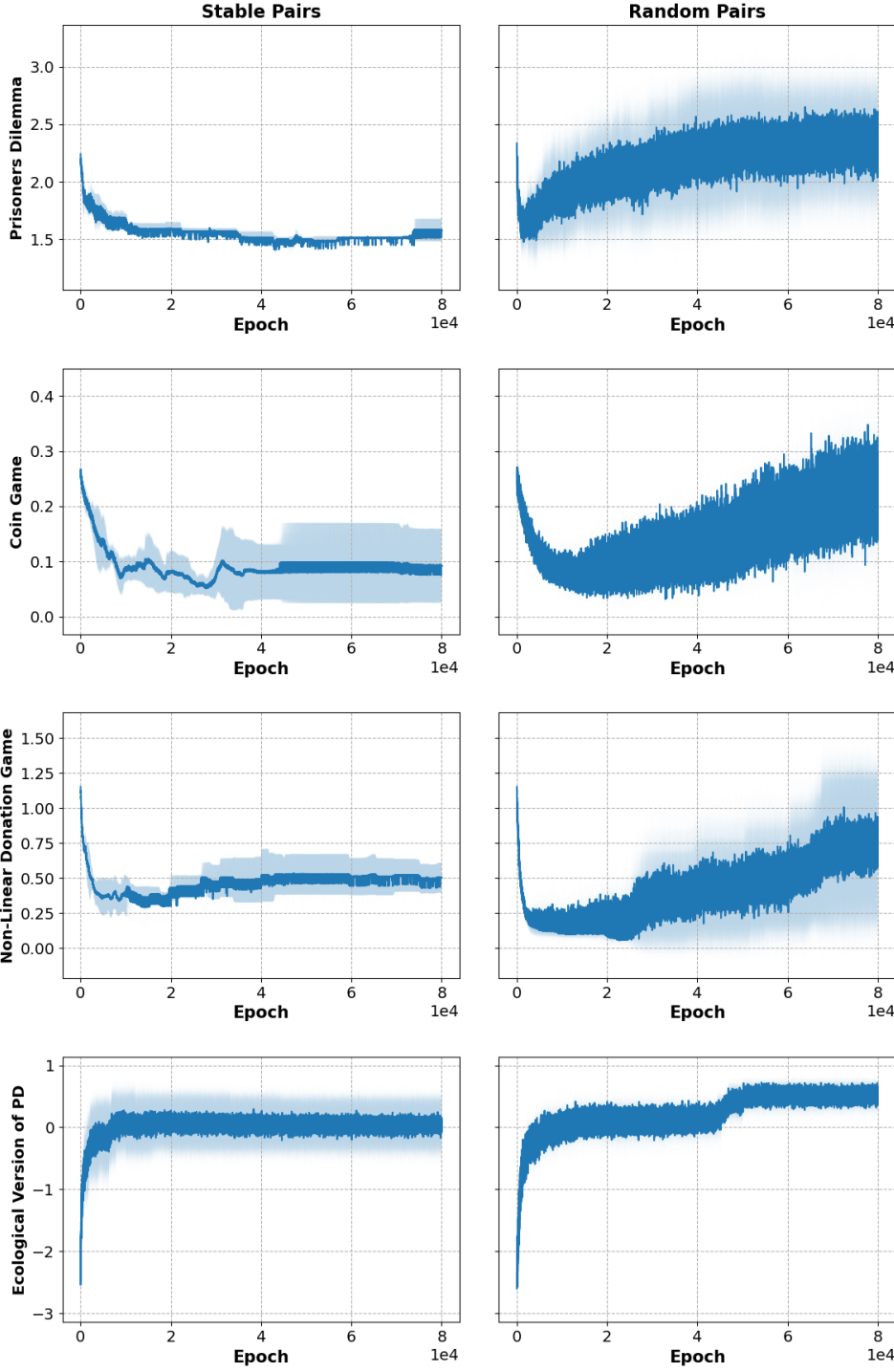


Figure 4: Impact of Interaction Stochasticity with Policy Gradients. A population of 50 agents with tabular, parameterized strategies was initialized using a Dirichlet (0.75, 0.75) distribution. We compare the performance of fixed pairings, where opponents remain fixed, with random pairings, where opponents are randomized each round. This figure illustrates that, even with the additional noise introduced by approximate policy gradient updates, random pairings can reverse defective outcomes. Despite the stochastic nature of strategy updates, population dynamics effectively guide agents toward cooperative equilibria.

621 frequently fail to sustain cooperation. We focus here on the random pairings setting, as the fixed
 622 pairings condition typically leads to rapid defection regardless of initialization, offering limited
 623 insight. This highlights the critical role of *initial behavioral diversity* in stabilizing outcomes, even
 624 under abstract function approximators like NNs.

625 This heightened sensitivity in neural networks (NNs) arises from the structural complexity of
 626 their parameter space. Unlike tabular strategies, which directly specify action probabilities, NNs
 627 encode these behaviors indirectly through a non-linear and high-dimensional weight vector θ .
 628 This added abstraction introduces a disconnect between the parameters being optimized and the
 629 resulting behavioral strategies, complicating the learning dynamics.

630 To formalize and visualize the disconnect between parameter updates and strategic behavior,
 631 the following distance metrics are defined:

- 632 • **NN parameter distance:** the normalized L^2 distance between the weight vectors θ of two
 633 neural network strategies.
- 634 • **Strategy (tabular) parameter distance:** the normalized L^2 distance between the action prob-
 635 ability distributions defined by two strategies.
- 636 • **Behavioral distance:**

$$D_{\text{behavior}}(\pi_i, \pi_k) = |V_{\text{avg}}(\pi_i, P) - V_{\text{avg}}(\pi_k, P)|, \quad (12)$$

637 where V_{avg} denotes the average performance of a strategy π against a fixed population P
 638 (see Section 4).

639 Since neural networks ultimately define tabular policies through their outputs, both the dis-
 640 tance between internal weight vectors (NN parameter distance) and the distance between result-
 641 ing action distributions (strategy parameter distance) can be measured. This dual representation
 642 enables analysis of how differences in NN parameters translate into behavioral differences.

643 To investigate this relationship, 2,000 strategies were sampled randomly and the above dis-
 644 tance metrics were computed for further analysis. ??a shows the relationship between NN pa-
 645 rameter distance and the corresponding strategy parameter distance, while ??b compares strategy
 646 parameter distance with behavioral distance across both representations.

647 ??a reveals a weak correlation between NN parameter distance and the corresponding tabular
 648 policy distance, highlighting the entangled nature of NN parameters. ??b further shows that
 649 tabular strategies maintain a stronger correlation between parameter and behavioral distances,
 650 whereas NN strategies exhibit little to no such alignment. This indicates that even minor changes
 651 in NN weights can result in large and unpredictable shifts in behavior.

652 This instability presents a key challenge for preserving behavioral diversity during learning.
 653 In NN-based systems, even a single training iteration can be sufficient to eliminate initial vari-
 654 ation. The challenge is amplified by the overparameterized and non-linear structure of the NN
 655 architecture. However, initializing neural strategies with low-concentration Dirichlet priors (e.g.,
 656 Dirichlet(0.5, 0.5)) promotes greater dispersion in parameter space, increasing the chance that
 657 agents converge to distinct local optima. Although the behavioral space is not directly controlled,
 658 this increased parameter-space variability can indirectly support a broader range of behaviors,
 659 helping to sustain diversity that would otherwise collapse early in training.

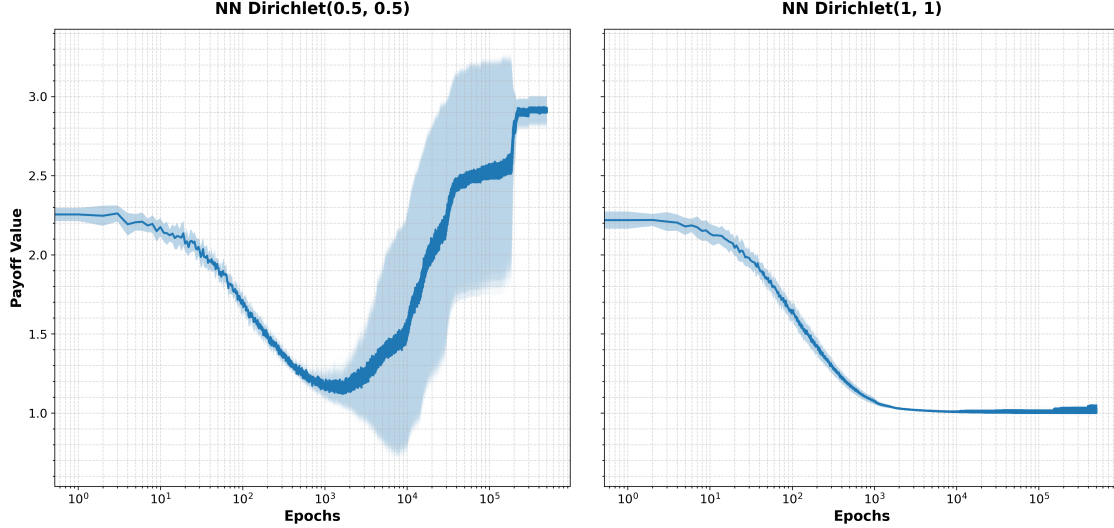


Figure 5: Parameterizing strategies with Neural Networks: A population of 50 agents is parameterized with neural network strategies using both Dirichlet (0.5, 0.5) and Dirichlet (1.0, 1.0). Exact gradients were used to update strategies. Cooperation is consistently achieved with a Dirichlet (0.5, 0.5) initialization, while it is unlikely with a Dirichlet (1.0, 1.0) initialization. Neural networks introduce complexities to the learning process, but these results indicate that cooperation remains attainable when parameters are appropriately tuned.

660 This sensitivity can be mitigated however, by using natural gradients. In continuous time, the
 661 natural gradient flow [33] uses the update $\frac{d\pi}{dt} = \nabla_{\pi} J(\pi)$, which corresponds to the learning dy-
 662 namics used in the tabular setting. On the other hand, the naïve gradient flow is $\frac{d\theta}{dt} = \nabla_{\theta} J(\pi^{\theta})$.
 663 Since $\frac{d\pi}{dt} = \frac{d\pi}{d\theta} \frac{d\theta}{dt}$ and $\nabla_{\theta} J(\pi^{\theta}) = \left(\frac{d\pi}{d\theta}\right)^{\top} \nabla_{\pi} J(\pi)$, the natural gradient gives the equation

$$\frac{d\theta}{dt} = \left(\left(\frac{d\pi}{d\theta} \right)^{\top} \frac{d\pi}{d\theta} \right)^{-1} \nabla_{\theta} J(\pi^{\theta}). \quad (13)$$

664 These learning dynamics account for the curvature of the parameterization via pulling back the
 665 metric tensor on the underlying Euclidean space.

666 5.5 Efficient optimization

667 Random pairings have been shown to mitigate defection, even under exact and approximate self-
 668-ish gradient updates. While these results have been validated in relatively simple Markov games,
 669 a natural question arises as to whether such findings scale to more complex, high-dimensional
 670 environments. To address this challenge, *Latent Reinforcement Learning* (LRL) is proposed, a novel
 671 framework enabling strategy optimization within a learned, low-dimensional latent embedding
 672 space.

673 Latent optimization techniques have been extensively applied in domains such as computer
 674 vision and natural language processing to facilitate more efficient learning by focusing on se-
 675 mantic meaningful, compressed representations. However, their application to multi-agent
 676 reinforcement learning, and specifically to strategy optimization in game-theoretic settings, is a
 677 significant advancement. The inherent non-stationarity and strategic interdependence of multi-

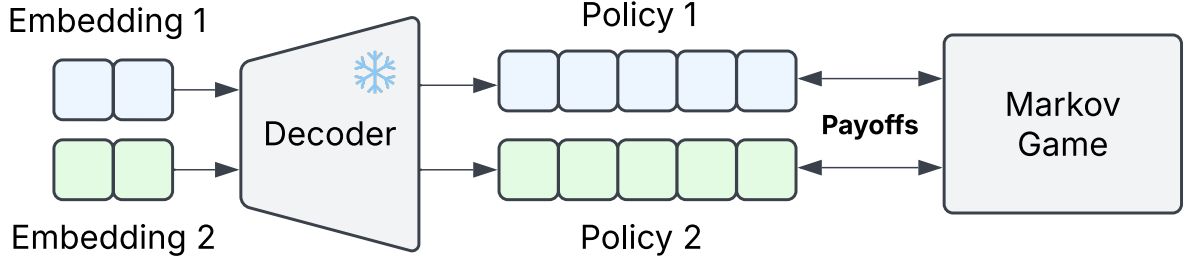


Figure 6: Latent Reinforcement Learning (LRL). LRL comprises two phases: (1) pre-training an autoencoder to learn compact strategy representations, using either parameter reconstruction or behavioral similarity, and (2) optimizing latent strategy embeddings directly. The encoder is discarded after initialization, while a frozen decoder maps latent embeddings back into full strategies deployed in the environment. Payoff gradients from interactions are backpropagated through the decoder, enabling stable and efficient optimization within the latent space.

678 agent environments make direct parameter optimization noisy and sample-inefficient. LRL pro-
 679 vides a promising approach by leveraging a structured latent space.

680 LRL operates in two stages. First, an autoencoder is trained to learn a compact and infor-
 681 mative representation of tabular strategies by minimizing reconstruction error. This yields an
 682 encoder E that maps strategies into a continuous latent space \mathbb{R}^d . Latent strategies are initialized
 683 by sampling from a Dirichlet distribution and encoding these samples:

$$z_0 \sim E(\text{Dirichlet}(\alpha)), \quad z_0 \in \mathbb{R}^d, \quad (14)$$

684 where z_0 denotes the initial latent embedding of the strategy. During the second stage, optimiza-
 685 tion proceeds directly in the latent space using gradient ascent updates:

$$z_{t+1} = z_t + \eta \nabla_{z_t} J(z_t), \quad (15)$$

686 where $J(z_t)$ represents the objective function evaluated on the decoded strategy corresponding
 687 to z_t . The decoder remains frozen during optimization, ensuring updates remain within the
 688 manifold of plausible strategies. An overview of the framework is illustrated in Figure 6.

689 A novel and compelling advantage emerges from integrating LRL with the BSAE, a com-
 690 bination not previously investigated. This integration combines the benefits of compact latent
 691 space optimization with the unique ability to optimize directly in behavior space, resulting in
 692 exceptional training efficiency. Beyond its immediate applications, this dual optimization frame-
 693 work has the potential to transform a wide range of RL problems. Existing approaches focus on
 694 parameter-space optimization, despite the fact that what truly matters is the resulting behavior.
 695 Since indirect optimization of behavior via parameters is often inefficient, this approach could
 696 open new pathways to faster, more interpretable, and more effective learning.

697 Results shown in Figure 7 demonstrate that latent optimization substantially improves sample
 698 efficiency, using the same parameters and x-axis scale as Figure 3 for a fair comparison. The au-
 699 toencoder effectively filters out high-frequency strategy details; for example, strategies differ-
 700 ing only in cooperation probability by small fractions such as 0.99 versus 0.9999 are nearly indistin-
 701 guishable in latent space. By abstracting away such fine-grained details, LRL guides learning
 702 toward behaviorally meaningful changes, reducing noise in gradient estimates and accelerating
 703 convergence.

704 The latent space functions as a form of structural regularization, much like how population
705 learning distributes learning pressure across diverse interactions. In LRL, this regularization
706 arises from dimensionality reduction, which restricts updates to a subspace capturing only the
707 most salient strategic features. Beyond improving sample efficiency, LRL provides a principled
708 mechanism for retaining the expressive capacity of neural networks while mitigating the adverse
709 effects of parameter sensitivity highlighted earlier. In high-dimensional NN weight spaces, small
710 perturbations can trigger abrupt, often erratic behavioral shifts, posing significant challenges
711 in non-stationary, multi-agent environments characterized by sharp local discontinuities. In con-
712 trast, latent optimization constrains learning to a smoother, low-dimensional manifold that filters
713 out noisy or redundant weight-level variation. This yields more behaviorally coherent updates
714 and stabilizes training dynamics.

715 6 Ablations and visualizations

716 6.1 Population size

717 To understand how population structure influences the emergence of cooperation, an ablation
718 study was conducted varying the population size from 2 to 50 in increments of 2. For each
719 population size, agent strategies were initialized by sampling from a Dirichlet distribution with
720 a concentration parameter of 0.75. This distribution ensures a moderate level of initial diversity,
721 preventing the population from starting in either highly uniform or overly chaotic configurations.
722 Each simulation was run until convergence, and results were averaged over 25 independent trials.
723 The average population reward is reported in Figure 8.

724 The results reveal that while small populations typically converge to defect-dominated out-
725 comes, populations as small as 10 begin to exhibit consistent convergence toward cooperative
726 equilibria. This trend becomes more robust as population size increases, with larger populations
727 reliably achieving high final rewards. Interestingly, the timescale of convergence remains largely
728 unaffected by population size. That is, while larger populations are more likely to discover coop-
729 erative strategies, they do not require more time to do so. These results have significant practical
730 implications suggesting that random interactions within a modestly sized and diverse group are
731 sufficient to reverse defection; unrealistically large populations are not required.

732 6.2 Diversity

733 There are two primary levers for increasing strategy coverage in a population: expanding popu-
734 lation size and modifying the diversity of initial strategy distributions. While larger populations
735 naturally span a broader region of the strategy space, a more direct and controllable method is
736 to adjust the Dirichlet concentration parameter used for initialization. In the previous section,
737 the effect of population size on cooperative convergence was explored. Here, the focus shifts to
738 how varying the Dirichlet concentration influences learning outcomes. To this end, a population
739 of 50 agents was initialized using concentration values in $\{0.25, 0.5, 0.75, 1.0, 1.25\}$, and learning
740 trajectories were examined across repeated trials and multiple games until convergence.

741 As shown in Figure 9, cooperative outcomes emerge reliably across a wide range of concen-
742 tration values. Interestingly, the most diverse setting (concentration = 0.25) produces the worst
743 performance, with final rewards significantly lower than in less diverse settings.

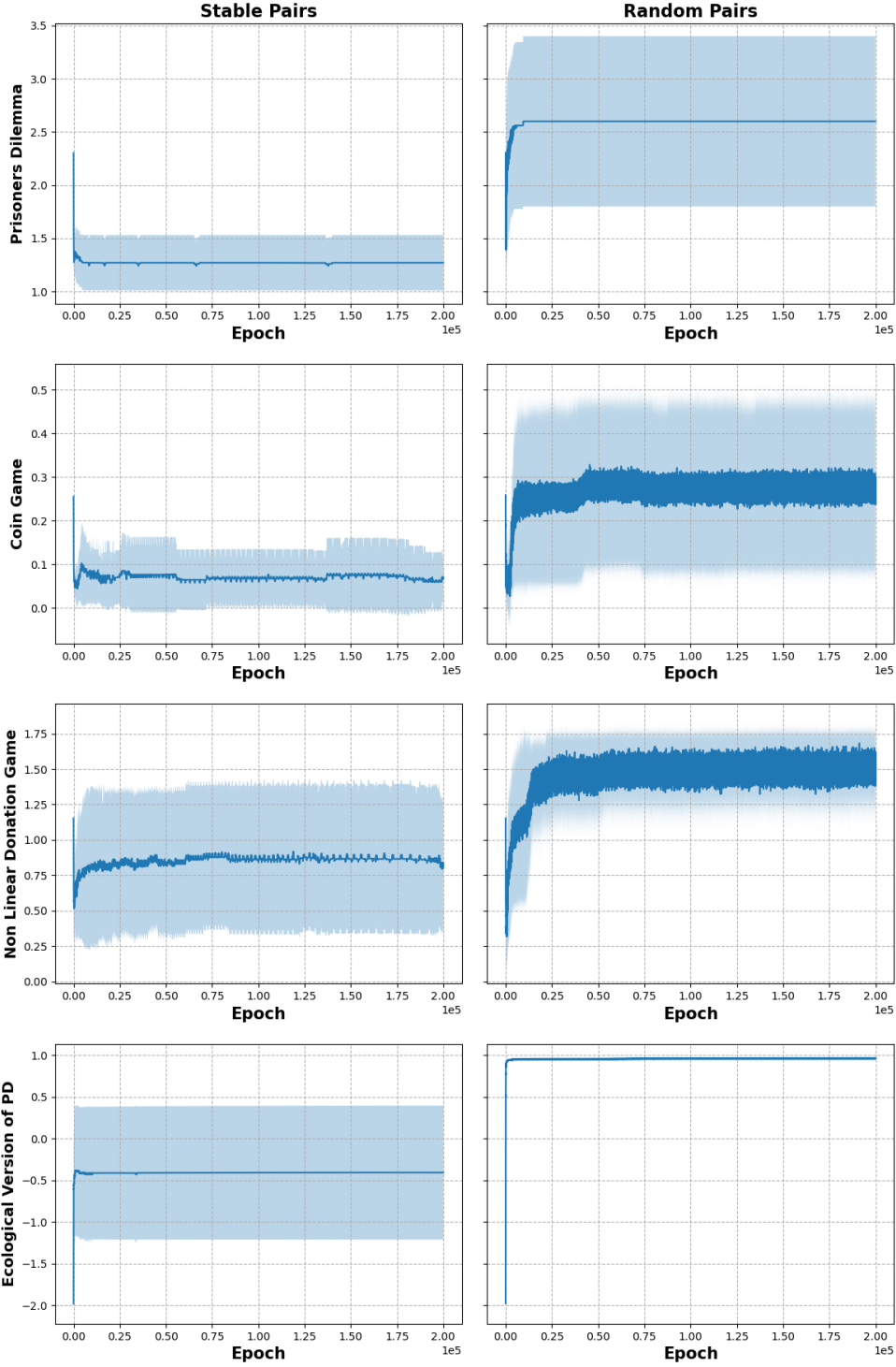


Figure 7: Impact of Latent Optimization on Sample Efficiency. Using the same parameters as in Figure 3, optimization is performed in the reduced latent space to enable a fair comparison. Latent optimization greatly enhances sample efficiency, with random pairings leading to rapid convergence toward cooperative outcomes, while fixed pairings remain prone to defection.

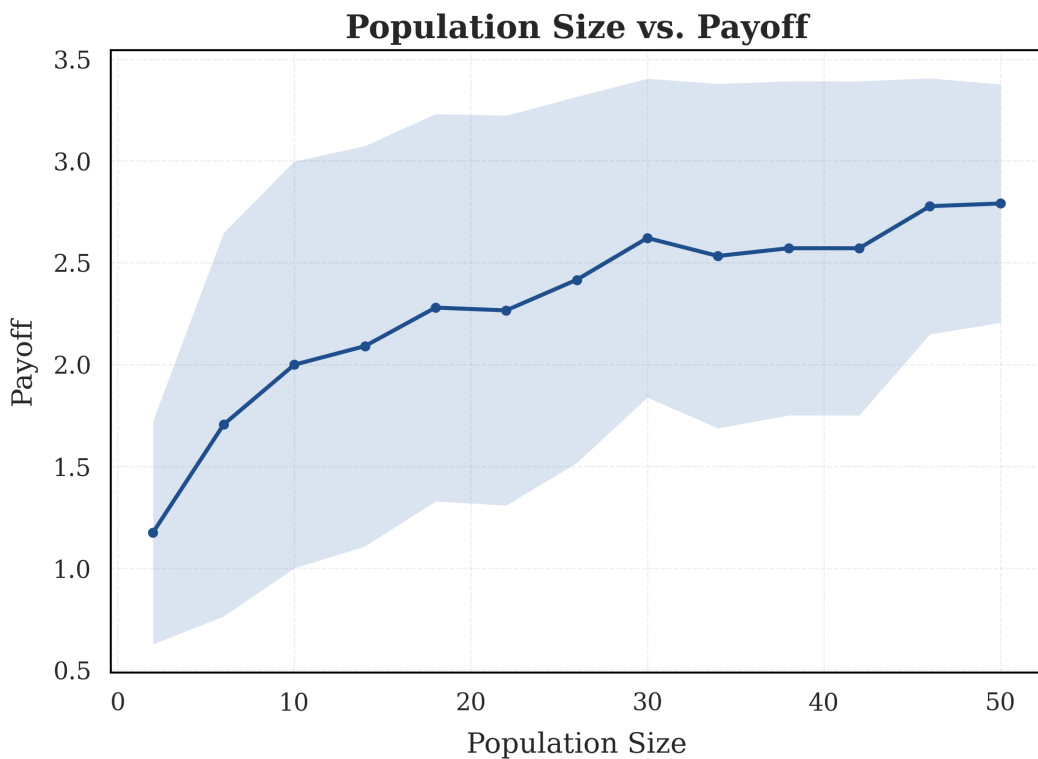


Figure 8: Influence of Population Size on Convergence Rewards: We investigate the impact of varying population sizes on the dynamics of cooperation. Each player in the population was initialized with strategies drawn from a Dirichlet (0.75, 0.75) distribution, and the population learning framework was run for up to 500,000 interactions or until convergence. Exact gradients were used to update strategies. The results show that larger populations support more robust convergence to cooperative equilibria.

744 To understand why excessive diversity can hinder learning in the IPD, consider how π_i would
745 update their strategy under each of the following conditions:

746 1. $\pi_i \approx 0, \pi_j \approx 0$ (Mutual Cooperation):

747 Mutual cooperation is stable and beneficial, leaving no incentive to change; gradients are
748 near zero.

749 2. $\pi_i \approx 0, \pi_j \approx 1$ (Sucker's Payoff):

750 The cooperator receives the lowest possible payoff ($S = 0$), but the gradient is also near
751 zero, providing no learning signal.

752 3. $\pi_i \approx 1, \pi_j \approx 0$ (Temptation):

753 The defector is highly rewarded and thus sees no reason to change, reinforcing selfish
754 behavior.

755 4. $\pi_i \approx 1, \pi_j \approx 1$ (Mutual Defection):

756 Although suboptimal, mutual defection is stable and offers no gradient incentive to coop-
757 erate.

758 In each of these cases, gradients either reinforce the same behavior or vanish. High initial di-
759 versity increases the likelihood that many agent pairs begin in one of these unproductive regions
760 of the strategy space. As a result, learning either stalls or exhibits unstable, oscillatory behavior.
761 This limitation is directly tied to the reward structure of the IPD, particularly the zero-valued
762 sucker's payoff, which fails to provide a gradient for improvement in crucial scenarios. If the
763 payoff matrix were altered (e.g., $S > 0$), these effects might be mitigated.

764 Another observation from Figure 9 is that as the Dirichlet concentration parameter increases,
765 reducing diversity, so too does the slope in the optimization trajectory. This indicates that with
766 higher initial concentrations, strategy behavior changes more readily. This pattern is consistent
767 with the nature of the initialized strategies: lower concentrations generate more extreme "confi-
768 dent" agents (near 0 or 1) that are difficult to shift through learning. In contrast, higher concentra-
769 tions produce more moderate "undecided" agents with strategies closer to the midpoint. These
770 undecided agents are more sensitive to learning signals and require fewer reinforcing updates to
771 shift toward a confident strategy, resulting in faster adaptation and a steeper optimization slope.

772 While diversity is generally beneficial, its effectiveness is highly dependent on the structure
773 of the environment. In poorly defined or weakly informative environments, such as those where
774 certain payoffs fail to produce meaningful learning signals, excessive initial diversity can lead
775 agents into unproductive regions of the strategy space. This, in turn, can hinder effective learning
776 and destabilize collective dynamics, ultimately impeding convergence toward optimal outcomes.

777 6.3 Visualization

778 To gain deeper insight into how population dynamics naturally foster cooperation in social dilem-
779 mas, the IPD is simulated over 100,000 iterations with a population of 50 agents. Agent strategies
780 are recorded every 100 epochs for subsequent analysis. In the IPD, memory-one strategies are
781 represented as five-dimensional vectors $(p_0, p_{CC}, p_{CD}, p_{DC}, p_{DD})$, where each component corre-
782 sponds to the probability of cooperating given the outcome of the previous round. To facilitate
783 interpretation, these high-dimensional vectors are projected into a two-dimensional space.

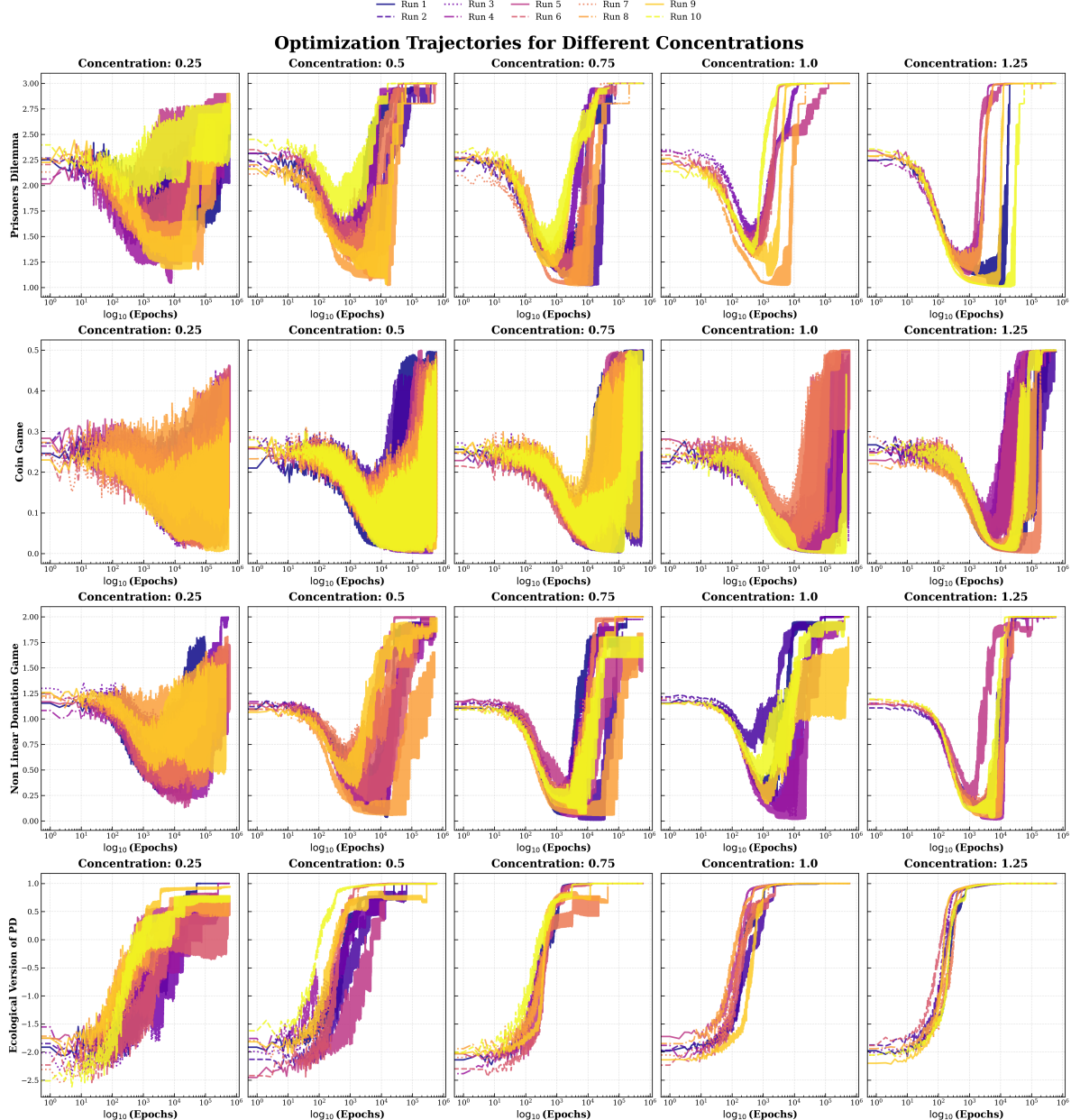


Figure 9: Effect of Initial Population Diversity on Equilibrium Rewards: We initialize a population of 50 agents with tabular, parameterized strategies, updating them using exact gradients. This figure demonstrates how the initial diversity of the population, controlled through the concentration parameters of the Dirichlet distribution, influences convergence rewards. Initial population diversity can have a big impact on the optimization trajectory.

784 While standard dimensionality reduction techniques such as Principal Component Analysis
785 (PCA) and t-distributed Stochastic Neighbor Embedding (t-SNE) are commonly used for such
786 tasks, they have notable limitations in this context. These methods typically rely on fixed, pre-
787 defined bases derived from the data distribution at a single point in time, such as the initial
788 population. However, as strategies adapt and evolve, these projections may lose interpretability.
789 Furthermore, these methods operate in parameter space and are agnostic to how strategies be-
790 have in practice; they do not capture how differences in parameters translate into differences in
791 outcomes.

792 To address these challenges, the behavior space autoencoder, introduced in previous sections,
793 is used to project policies into a behaviorally meaningful two-dimensional space. Recall that
794 this model is trained using pairs of strategies sampled from a Dirichlet (0.5, 0.5) distribution,
795 ensuring diverse and representative coverage of the strategy space. Each strategy is encoded
796 into a low-dimensional latent vector, and the decoder predicts the expected payoffs when the
797 two strategies interact in the IPD. The model is optimized to minimize the discrepancy between
798 these predicted rewards and the true game-theoretic payoffs. This training objective ensures
799 that the latent space reflects behavioral equivalence: strategies that perform similarly, regardless
800 of their parameterization, are embedded near each other. Crucially, these embeddings remain
801 meaningful under any distribution of population strategies.

802 This approach constitutes a novel contribution to the analysis of evolving strategic behavior.
803 By grounding the projection space in observed behavioral consequences rather than structural
804 similarity, the behavior space autoencoder provides a consistent and interpretable framework for
805 understanding complex dynamics in policy evolution. Unlike static techniques, it retains inter-
806 pretability across time, even as the population distribution shifts dramatically. Beyond the spe-
807 cific context of the IPD, this methodology offers a general and flexible tool for interpretability in
808 dynamic multi-agent systems. The same principles can be applied to a wide variety of domains,
809 including reinforcement learning, evolutionary games, policy space exploration, and real-world
810 multi-agent coordination problems. By providing a way to visualize and analyze agent behavior,
811 the behavior space autoencoder opens new pathways for understanding and guiding emergent
812 behavior in complex adaptive systems.

813 The trained encoder is leveraged to visualize the evolving landscape of strategies through-
814 out the simulation. A complete visualization of the full evolutionary trajectory is provided in
815 the supplementary material, while a selection of representative snapshots is presented in ???. In
816 these figures, each agent's strategy is depicted as a blue point embedded in the learned two-
817 dimensional behavior space. To provide behavioral context and aid interpretation, canonical
818 reference strategies, such as Tit-for-Tat (TFT), Always Cooperate (ALLC), Always Defect (ALLD),
819 and Generous Tit-for-Tat (GTFT), are also plotted. These strategies serve as well-known behav-
820 ior archetypes: TFT initiates with cooperation and then reciprocates the opponent's previous
821 action, promoting mutual cooperation; ALLC cooperates unconditionally, leaving it vulnerable
822 to exploitation; ALLD defects unconditionally, representing a purely selfish approach; and GTFT
823 modifies TFT by occasionally forgiving defections, thus helping sustain cooperation even in noisy
824 or error-prone environments.

825 The visualization reveals that the initial population is highly diverse, exploring a broad region
826 of the strategy space. However, within the first few hundred epochs, the population dynamics
827 lead the distribution to drift toward ALLD and cluster within a region characterized by extor-
828 tionate strategies. These extortionate strategies consistently punish defectors but also defect with

829 some probability against cooperators, exploiting them for gain. Crucially, these strategies exhibit
830 negative reinforcement: when two extortionate strategies interact, the selfish-learning gradients
831 push both toward increasingly defecting behaviors, ultimately converging on ALLD. A similar
832 pattern emerges when extortionate strategies are paired with TFT; despite TFT’s reciprocity, both
833 agents tend to evolve toward defection in response to exploitation.

834 Escaping these defectionary feedback loops requires sufficient population diversity. In partic-
835 ular, forgiving strategies, characterized by high probabilities of cooperating following an oppo-
836 nent’s defection (high p_{CD}), play a pivotal role in redirecting the learning dynamics of extortio-
837 nate strategies toward more cooperative outcomes. While these forgiving strategies are vulnerable
838 to exploitation in the short term, they are rewarded over a longer horizon as they serve to shift
839 the population toward cooperative dynamics. Importantly, with enough diversity, these forgiving
840 strategies naturally emerge through random interactions.

841 When player pairings are fixed, agents learn exclusively from repeated interactions with the
842 same partner, limiting their exposure to diverse behaviors. If both agents fall into a mutual de-
843 fection pattern, there are no external influences to break the cycle, making full defection (ALLD)
844 a likely outcome. While cooperation is not impossible under these conditions, it tends to be rare
845 and fragile. In contrast, when agents are randomly paired across the population, they are contin-
846 ually exposed to new behaviors. This variety introduces opportunities to escape local defection
847 traps and promotes the discovery and reinforcement of cooperative strategies.

848 This study reveals that forgiving strategies, those that offer opportunities for recovery af-
849 ter defection, can fundamentally reshape learning dynamics in multi-agent systems. In MARL
850 settings, such strategies provide a stabilizing force that prevents convergence to degenerate out-
851 comes. In systems with many agents, such as swarm robotics, decentralized energy grids, or
852 financial trading platforms, missteps and exploitation are inevitable. Forgiving strategies allow
853 agents to absorb occasional adversarial behavior without collapsing into permanent mistrust or
854 retaliation. This creates space for cooperation to recover and persist. From a systems design
855 perspective, incorporating mechanisms that promote or incentivize forgiveness, such as reward
856 shaping, memory-based policies, or structured exploration, can help unlock more resilient co-
857 operative equilibria. This insight also bridges to broader societal systems, where forgiveness
858 underlies everything from diplomatic treaties to community conflict resolution, reinforcing its
859 importance as a universal lever for long-term coordination.

860 7 Discussion

861 The central finding is that randomized interactions among selfish agents reverse defectionary out-
862 comes, a result that contradicts prior literature, which points to the fact that stochastic pairings
863 invariably degrade cooperation. In a diverse set of simple Markov games designed to capture
864 a wide range of realistic social dilemmas, agents matched with randomly drawn opponents not
865 only learn to cooperate but also reliably converge to the optimal strategy. Rather than serving
866 as a barrier, population-level stochasticity produces forgiving strategies that act as attractors in
867 the strategic landscape, drawing defectors back into cooperative clusters and guiding the entire
868 population toward mutually beneficial, optimal outcomes, achieved without any engineered in-
869 terventions such as reward shaping, partner selection, or centralized coordination. Randomized
870 interactions serve as a natural mechanism for robust optimization, enabling selfish agents to
871 develop strategies that perform reliably in the context of conflicting goals.

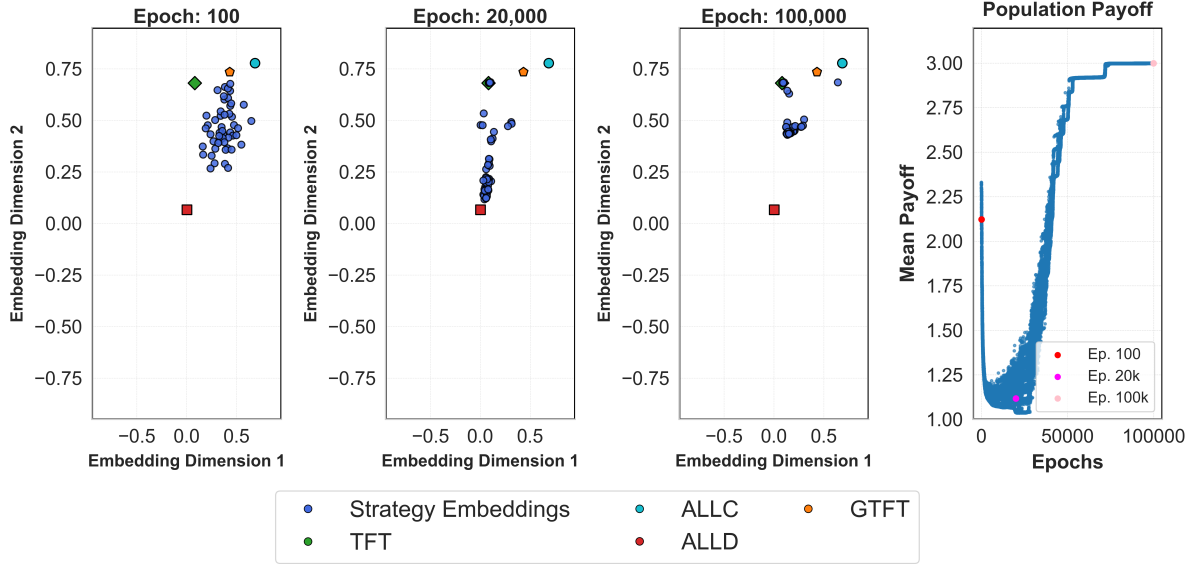


Figure 10: Evolving Strategy Landscape. A sequence of snapshots illustrates the trajectory of agent embeddings over training time. Initially, the population is highly diverse, exploring a wide range of strategies. By epoch 20,000, extortionist strategies dominate, leading to lower overall payoffs. However, diversity persists, and the presence of forgiving strategies creates gradients that shift the population toward cooperation. By epoch 100,000, most agents have moved away from ALLD, converging toward more forgiving, prosocial behaviors. This evolution underscores the role of transient interactions in shaping long-term dynamics and highlights how self-interested learning can lead to cooperative outcomes.

872 The behavior space autoencoder is a truly novel advance in strategy representation. Unlike
 873 conventional dimensionality-reduction methods, such as principal component analysis, that rely
 874 on a fixed basis and can quickly become obsolete as strategy distributions evolve, the BSAE
 875 learns latent embeddings directly from empirical payoff data. This behavior-centric approach
 876 ensures that the representation remains meaningful even as new strategies emerge, clustering
 877 them by functional payoff outcomes rather than superficial parameter similarities. As a result, the
 878 BSAE not only makes it possible to visualize the strategic landscape but also provides a robust
 879 foundation for subsequent optimization techniques that exploit these learned latent spaces to
 880 accelerate convergence and improve sample efficiency.

881 Latent optimization techniques have become widespread in machine learning, yet their ap-
 882 plication to game-theoretic multi-agent reinforcement learning remains novel. This work shows
 883 that even optimizing simple parameter-space embeddings with Latent Reinforcement Learning
 884 (LRL) yields strong gains in sample efficiency. However, when combined with the behavior space
 885 autoencoder (BSAE), the benefits are amplified: first uncovering the geometry of strategy space
 886 and then performing optimization directly within that manifold, this integrated framework shifts
 887 multi-agent reinforcement learning away from blind parameter search toward behavior-aligned
 888 learning, dramatically increasing sample efficiency.

889 Beyond overturning longstanding assumptions in multi-agent reinforcement learning, these
 890 findings reveal a broader design principle for decentralized, heterogeneous systems: random-
 891 ness, when combined with behavior-aware learning, can cultivate resilient cooperation. This
 892 insight carries significant implications for robotics and autonomous systems. Multi-robot teams
 893 and autonomous vehicle fleets frequently depend on carefully engineered coordination proto-

894 cols that often falter when faced with real-world variability. Introducing randomized encoun-
895 ters among agents provides a more flexible and adaptive approach, enabling systems to organi-
896 cally discover robust, cooperative behaviors without explicit programming. For instance, in
897 autonomous traffic systems, vehicles interacting with a diverse and unpredictable set of partners
898 may naturally develop forgiving strategies that help maintain smooth flow and safety, even when
899 individual agents occasionally make errors. Similarly, in distributed computing or peer-to-peer
900 networks, random peer selection can promote tolerant behaviors, such as accepting intermittent
901 packet loss, that sustain overall system integrity amid decentralization and noise. In these con-
902 texts, randomness does not breed chaos but instead guides systems toward globally beneficial
903 outcomes that rigid, pre-scripted solutions frequently fail to achieve.

904 This dynamic echoes across numerous disciplines. In ecology, random disturbances prevent
905 any single species from dominating resources, thereby preserving biodiversity and maintaining
906 ecosystem resilience. Similarly, random interactions within agent populations break up uni-
907 form defection, enabling cooperative strategies to persist, propagate, and ultimately prevail. In
908 economics, decentralized markets often depend on random buyer-seller pairings, where trust
909 is cultivated not through heavy regulation but through repeated, diverse interactions, fostering
910 forgiving norms such as leniency following minor defaults. Sociology reveals comparable pat-
911 terns, where cooperation and forgiveness arise organically from informal, stochastic exchanges,
912 like gossip, reputation building, and interpersonal negotiation, rather than from top-down man-
913 dates. Political science further reinforces this insight: truth and reconciliation processes deliber-
914 ately introduce unpredictable pairings to disrupt cycles of conflict and rebuild social cohesion.
915 Across these varied fields, randomness acts as a catalyst for flexibility, diversity, and the emer-
916 gence of stable cooperative norms. These same principles hold true in artificial systems, where
917 forgiving strategies spontaneously emerge through diverse encounters, serving as powerful sta-
918 bilizers within complex, decentralized environments. Despite these promising insights, several
919 important limitations should be acknowledged. The results are derived from relatively simple
920 stochastic environments, games defined by memory-one strategies and clear payoff structures.
921 While such settings effectively isolate core social dilemmas, they abstract away many complexi-
922 ties inherent to real-world multi-agent systems. Domains with continuous action spaces, partial
923 observability, asynchronous decision-making, or large, heterogeneous populations present open
924 challenges not addressed in this work. Scalability, in particular, remains a central concern, as the
925 computational burden of modeling and optimizing over increasingly rich strategy spaces grows
926 rapidly. Nonetheless, the integration of the behavior space autoencoder (BSAE) with Latent Re-
927 inforcement Learning (LRL) offers a potential path forward. By enabling direct optimization
928 within a compressed, behaviorally meaningful latent space, this framework can dramatically re-
929 duce sample complexity and improve learning efficiency, making it a promising foundation for
930 scaling cooperation dynamics to more complex and realistic environments.

931 Several promising avenues for future research arise from this work. One key direction is to ex-
932 plore how forgiving strategies can be systematically introduced into existing populations to shift
933 their dynamics toward more cooperative and socially beneficial outcomes. Understanding how
934 to guide populations toward forgiveness could have broad implications for designing resilient
935 multi-agent systems in economics, robotics, and distributed computing. Another important area
936 is investigating the impact of different social network structures on cooperation dynamics. Since
937 real-world interactions are rarely fully random, studying how network topology influences the
938 emergence and stability of cooperative behaviors can inform the design of more effective decen-

939 tralized systems and social platforms. Finally, a particularly timely direction is examining how
940 populations of self-interested large language models (LLMs) behave when faced with conflicts
941 of interest. Understanding whether and how population-level dynamics encourage cooperation
942 among LLMs is crucial as these models are increasingly deployed in settings requiring negotia-
943 tion, collaboration, or conflict resolution. Insights here could help ensure that AI systems align
944 better with human values and collective goals.

945 **Code availability**

946 Implementation details may be found at https://github.com/smerrillunc/population_learning.

947 **References**

- 948 [1] L. Chen, P. Deng, L. Li, and X. Hu, “Mixed motivation driven social multi-agent reinforce-
949 ment learning for autonomous driving”, IEEE/CAA Journal of Automatica Sinica **12**, 1272–
950 1282 (2025).
- 951 [2] R. Zhang, J. Hou, F. Walter, S. Gu, J. Guan, F. Röhrbein, Y. Du, P. Cai, G. Chen, and A. Knoll,
952 *Multi-Agent Reinforcement Learning for Autonomous Driving: A Survey*, 2024.
- 953 [3] S. Sarin, S. K. Singh, S. Kumar, S. Goyal, B. B. Gupta, W. Alhalabi, and V. Arya, “Unleash-
954 ing the power of multi-agent reinforcement learning for algorithmic trading in the digital
955 financial frontier and enterprise information systems”, Computers, Materials and Continua
956 **80**, 3123–3138 (2024).
- 957 [4] I. Maeda, D. deGraw, M. Kitano, H. Matsushima, H. Sakaji, K. Izumi, and A. Kato, “Deep
958 reinforcement learning in agent based financial market simulation”, Journal of Risk and
959 Financial Management **13**, 71 (2020).
- 960 [5] Z. Xiong, B. Luo, B.-C. Wang, X. Xu, X. Liu, and T. Huang, “Decentralized multiagent rein-
961 forcement learning based state-of-charge balancing strategy for distributed energy storage
962 system”, IEEE Transactions on Industrial Informatics **20**, 12450–12460 (2024).
- 963 [6] X. Fang, J. Wang, G. Song, Y. Han, Q. Zhao, and Z. Cao, “Multi-agent reinforcement learning
964 approach for residential microgrid energy scheduling”, Energies **13**, 123 (2019).
- 965 [7] T. Roughgarden, *Selfish routing and the price of anarchy* (The MIT Press, 2005).
- 966 [8] J. Hu and M. P. Wellman, “Nash q-learning for general-sum stochastic games”, Journal of
967 Machine Learning Research **4**, 1039–1069 (2003).
- 968 [9] J. P. Agapiou, A. S. Vezhnevets, E. A. Duéñez-Guzmán, J. Matyas, Y. Mao, P. Sunehag, R.
969 Köster, U. Madhushani, K. Kopparapu, R. Comanescu, et al., *Melting pot 2.0*, 2022.
- 970 [10] T. W. Sandholm and R. H. Crites, “Multiagent reinforcement learning in the iterated pris-
971 oner’s dilemma”, Biosystems **37**, 147–166 (1996).

972 [11] P. Barnett and J. Burden, "Oases of cooperation: an empirical evaluation of reinforcement
 973 learning in the iterated prisoner's dilemma", in Proceedings of the workshop on artifi-
 974 cial intelligence safety 2022 (safeai 2022) co-located with the thirty-sixth aaai conference
 975 on artificial intelligence (aaai2022), Vol. 3087, edited by G. Pedroza, J. Hernández-Orallo,
 976 X. C. Chen, X. Huang, H. Espinoza, M. Castillo-Effen, J. McDermid, R. Mallah, and S. Ó
 977 hÉigearthaigh, CEUR Workshop Proceedings (2022).

978 [12] E. M. de Cote, A. Lazaric, and M. Restelli, "Learning to cooperate in multi-agent social
 979 dilemmas", in Proceedings of the fifth international joint conference on autonomous agents
 980 and multiagent systems, AAMAS '06 (2006), pp. 783–785.

981 [13] Y. Shoham, R. Powers, and T. Grenager, "If multi-agent learning is the answer, what is the
 982 question?", *Artificial Intelligence* **171**, 365–377 (2007).

983 [14] J. Z. Leibo, V. Zambaldi, M. Lanctot, J. Marecki, and T. Graepel, *Multi-agent reinforcement
 984 learning in sequential social dilemmas*, 2017.

985 [15] E. Hughes, J. Z. Leibo, M. Phillips, K. Tuyls, E. Dueñez-Guzman, A. García Castañeda,
 986 I. Dunning, T. Zhu, K. McKee, R. Koster, et al., "Inequity aversion improves cooperation
 987 in intertemporal social dilemmas", in Advances in neural information processing systems,
 988 Vol. 31 (2018).

989 [16] U. Madhushani, K. R. McKee, J. P. Agapiou, J. Z. Leibo, R. Everett, T. Anthony, E. Hughes,
 990 K. Tuyls, and E. A. Duéñez-Guzmán, *Heterogeneous social value orientation leads to meaningful
 991 diversity in sequential social dilemmas*, 2023.

992 [17] E. A. Duéñez-Guzmán, R. Comanescu, Y. Mao, K. R. McKee, B. Coppin, S. Sadedin, S. Chi-
 993 appa, A. S. Vezhnevets, M. A. Bakker, Y. Bachrach, W. Isaac, K. Tuyls, and J. Z. Leibo, "Per-
 994 ceptual interventions ameliorate statistical discrimination in learning agents", *Proceedings
 995 of the National Academy of Sciences* **122**, e2319933121 (2025).

996 [18] K. R. McKee, X. Bai, and S. T. Fiske, "Warmth and competence in human-agent coopera-
 997 tion", *Autonomous Agents and Multi-Agent Systems* **38**, 23 (2024).

998 [19] E. Bahel, S. Ball, and S. Sarangi, "Communication and cooperation in prisoner's dilemma
 999 games", *Games and Economic Behavior* **133**, 126–137 (2022).

1000 [20] E. M. de Cote, A. Lazaric, and M. Restelli, "Learning to cooperate in multi-agent social
 1001 dilemmas", in Proceedings of the fifth international joint conference on autonomous agents
 1002 and multiagent systems, AAMAS '06 (2006), pp. 783–785.

1003 [21] W. Barfuss and J. M. Meylahn, "Intrinsic fluctuations of reinforcement learning promote
 1004 cooperation", *Scientific Reports* **13**, 10.1038/s41598-023-27672-7 (2023).

1005 [22] J. Foerster, R. Y. Chen, M. Al-Shedivat, S. Whiteson, P. Abbeel, and I. Mordatch, "Learning
 1006 with Opponent-Learning Awareness", in Proceedings of the 17th international conference
 1007 on autonomous agents and multiagent systems, AAMAS '18 (2018), pp. 122–130.

1008 [23] M. Babes, E. M. de Cote, and M. L. Littman, "Social reward shaping in the prisoner's
 1009 dilemma", in Proceedings of the 7th international joint conference on autonomous agents
 1010 and multiagent systems - volume 3, AAMAS '08 (2008), pp. 1389–1392.

1011 [24] R. Lowe, Y. Wu, A. Tamar, J. Harb, P. Abbeel, and I. Mordatch, *Multi-agent actor-critic for
 1012 mixed cooperative-competitive environments*, 2017.

1013 [25] W. Barfuss and J. M. Meylahn, "Intrinsic fluctuations of reinforcement learning promote
1014 cooperation", *Scientific Reports* **13**, 10.1038/s41598-023-27672-7 (2023).

1015 [26] M. L. Littman, "Friend-or-Foe Q-learning in General-Sum Games", in *Proceedings of the*
1016 *eighteenth international conference on machine learning* (2001), pp. 322–328.

1017 [27] A. McAvoy, Y. Mori, and J. B. Plotkin, "Selfish optimization and collective learning in
1018 populations", *Physica D: Nonlinear Phenomena* **439**, 133426 (2022).

1019 [28] N. Anastassacos, S. Hailes, and M. Musolesi, "Partner selection for the emergence of co-
1020 operation in multi-agent systems using reinforcement learning", *Proceedings of the AAAI*
1021 *Conference on Artificial Intelligence* **34**, 7047–7054 (2020).

1022 [29] C.-w. Leung and P. Turrini, "Learning partner selection rules that sustain cooperation in
1023 social dilemmas with the option of opting out", in *Proceedings of the 23rd international*
1024 *conference on autonomous agents and multiagent systems, AAMAS '24* (2024), pp. 1110–
1025 1118.

1026 [30] L. S. Shapley, "Stochastic games", *Proceedings of the National Academy of Sciences* **39**,
1027 1095–1100 (1953).

1028 [31] A. Lerer and A. Peysakhovich, *Maintaining cooperation in complex social dilemmas using deep*
1029 *reinforcement learning*, 2017.

1030 [32] R. S. Sutton, D. McAllester, S. Singh, and Y. Mansour, "Policy gradient methods for re-
1031 inforcement learning with function approximation", in *Advances in neural information*
1032 *processing systems*, Vol. 12, edited by S. Solla, T. Leen, and K. Müller (1999).

1033 [33] W. Li and G. Montúfar, "Natural gradient via optimal transport", *Information Geometry* **1**,
1034 181–214 (2018).